Biophysical Chemistry 5 (1976) 137–157

SEDIMENTATION EQUILIBRIUM OF PROTEINS IN DENSITY GRADIENTS *

James B. IFFT
Department of Chemistry, University of Redlands, Redlands, California 92373, USA

The technique of sedimentation equilibrium in density gradients in the analytical ultracentrifuge has been applied to the study of proteins. A variety of effects and procedures including the use of density marker beads, the effects of pressure on buoyant density and pH, and the calculation of compositional density gradient proportionality constants and density–refractive index relations have been developed. The buoyant densities of twenty-four proteins have been measured and hydration values computed. The buoyant titrations of six proteins have been measured. These data have been interpreted in terms of the buoyant titrations which have been obtained for six ionizable homopolypeptides, five copolypeptides, two non-ionizable homopolypeptides and three chemically modified proteins. Spectropolarimetry and potentiometric titrations were employed to further interpret these data. Approximate values for dissociation constants, numbers of ionizable residues, and the nature of ions bound or dissociated upon ionization have been obtained. The relation between potentiometric and buoyant titrations and the use of density gradient centrifugation as a probe for protein structure have been explored.

1. Introduction

This symposium honors the pioneering work of The Svedberg fifty years ago at the University of Uppsala in Sweden. Professor Svedberg and his coworkers conceived, constructed and tested an analytical ultracentrifuge. Among a number of important contributions, they provided convincing evidence that proteins consist of discrete collections of atoms having definite size and shape; hemoglobin was found to be a "monodisperse colloid". A rich history of important contributions to a variety of polymer studies has evolved from this early work.

One of these developments was the exciting discovery eighteen years ago in Professor Vinograd's laboratory of the technique of sedimentation equilibrium in a density gradient. Meselson, Stahl and Vinograd [1] provided a description of the method, some preliminary data, and the initial thermodynamic derivations required to understand these experiments. The replication experiments of Meselson and Stahl [2] and the finding by Doty [3] and others of the linear relationship between buoyant density and G–C content were early classic experiments. These experiments have been extended in a variety of directions up to the recent demonstration by Hearst and Schmid [4] that measurements in density gradients yield correct molecular weights for a number of phage DNAs. It is apparent from these few examples that most of the applications of this technique have been in the study of nucleic acids.

Professor Vinograd and I [5,6] began a study of the applications of this technique to an understanding of the properties of proteins in 1957. This work has been continued in our modest laboratory at the University of Redlands up to the present time. All of the research results reported in this paper have been obtained by undergraduate students. Among the students who have contributed to the work discussed in this paper are Allan Williams, James Ritchey, John Zil, William Martin, Kathleen Kinzie, Lawrence Lum, Robert Almassy, Dan Sharp, David Ellis, Valerie Coffman, Joseph Geleris, Dale Thorpe, and John Ruark. This work has been reviewed in part elsewhere [7–9].

The early work in Professor Vinograd's laboratory centered around a study of the techniques required to

* This work was supported in part by a research grant from the National Institute of General Medical Sciences (GM 18871), National Institutes of Health, U.S. Public Health Service.

obtain the correct anhydrous molecular weight of one well-characterized protein, bovine serum mercaptalbumin, BMA. It was found necessary to measure the buoyant properties of BMA in a variety of salt solutions. All measurements were made at one pH, the isoelectric point of this protein.

Much of the work of our laboratory has involved the relaxation of the restrictions involved in this early work. A variety of proteins have been examined. Buoyant titrations, the measurement of the buoyant density over a range of pH's, have been measured for a number of proteins as well as a series of homo- and copolypeptides.

2. Recent developments in technique

2.1. Multicell runs

The initial work with this technique for the study of proteins was done in An–D rotors. This permitted the use of either one or two cells, using a negative wedge in the latter case (figs. 1 and 2). Because so many data points are required to generate a buoyant titration curve and because of the time and increasing expense of each run, we now utilize the 4-cell An–F aluminum and titanium rotors in most of our density gradient work. This permits the use of three cells plus a counterbalance or 4 cells, accompanied by the use of the outer reference hole in the rotor. Wedge combinations ranging from +1 down to −2 have been found to be successful for four-cell runs. Fig. 3 provides a nice demonstration of the quality of the schlieren image obtainable in a 4-cell run [10]. Factors which can complicate such runs are overlapping menisci or precipitated bands in one cell obscuring a crucial region of another solution.

2.2. Investigation of marker beads for measurement of buoyant density

The study of proteins in density gradients up to this time has relied on the thermodynamic calculation

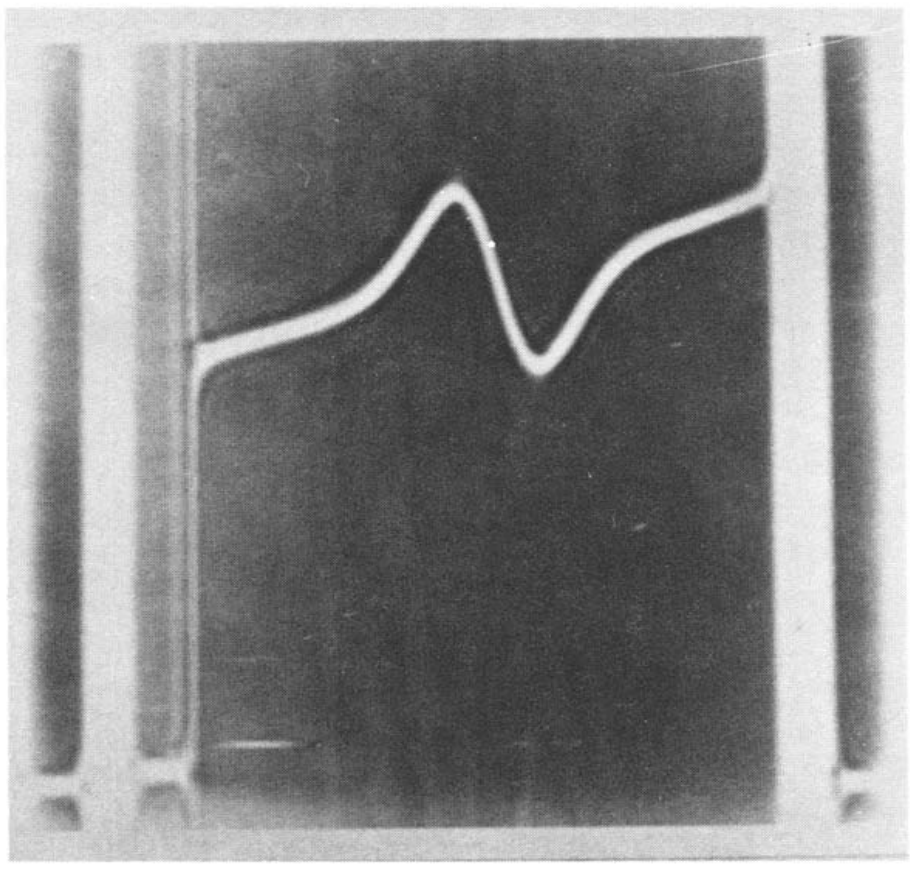

Fig. 1. Equilibrium schlieren photograph of 0.1% BMA in CsCl of ρ_c = 1.279 g/ml, pH = 5.08, acetate buffer (μ = 0.01) at 56 100 rpm and 25°C. Single sector, 4°, Kel–F centerpiece.

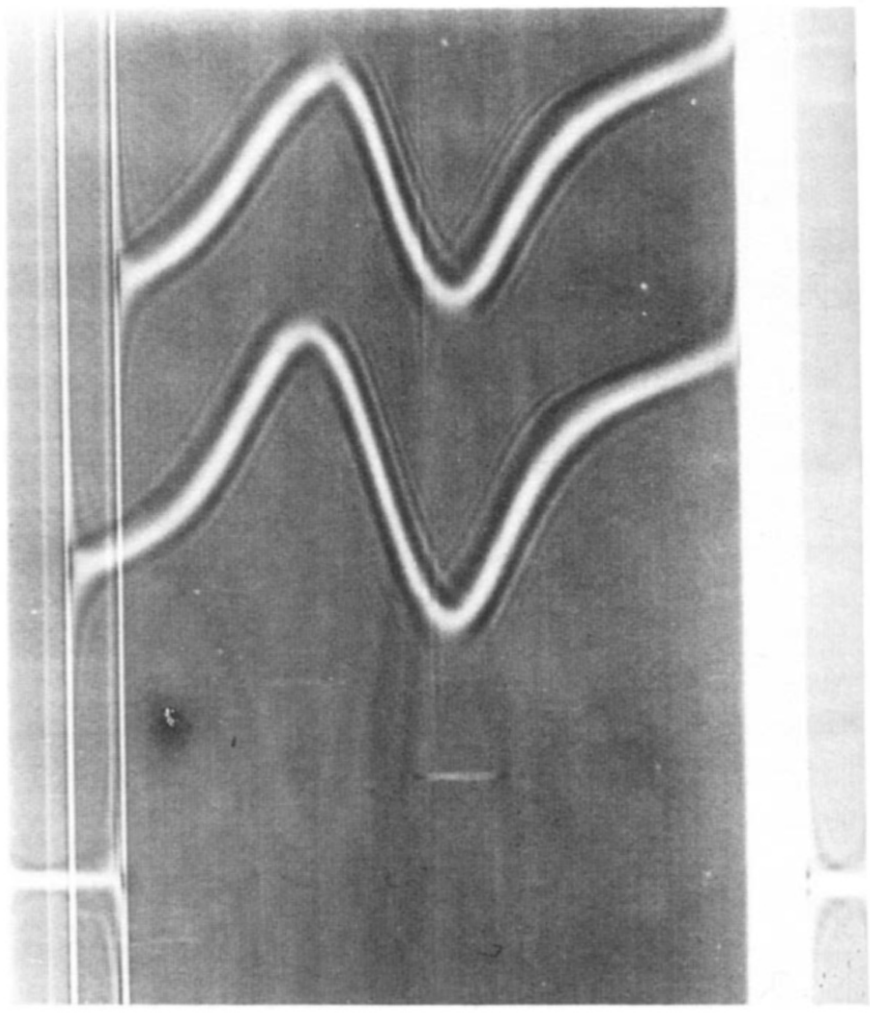

Fig. 2. Equilibrium schlieren photograph of a two-cell run with 0.1% BMA in CsCl at the isoelectric point in each cell. Angular velocity was 56 100 rpm and 25°C. Single sector, 4°, Kel–F centerpiece.

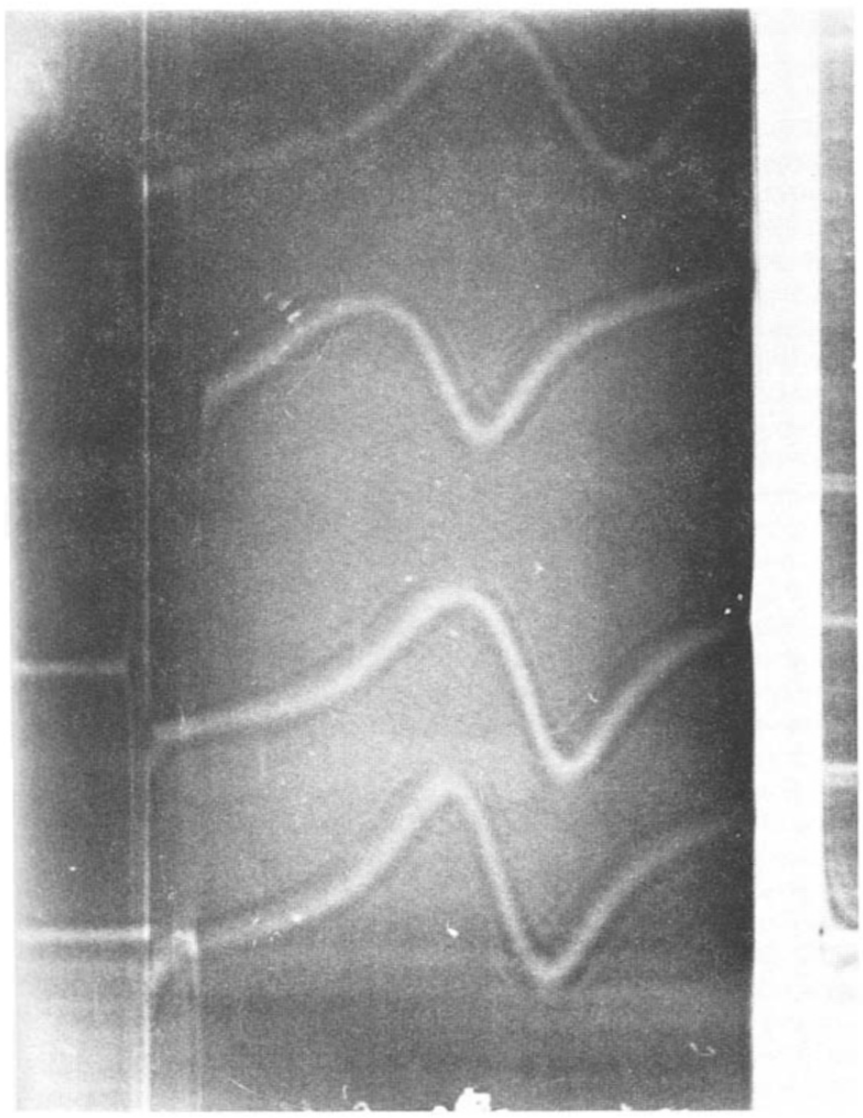

Fig. 3. Equilibrium schlieren photograph of four cells containing respectively from top to bottom: +1°, native BMA; 0°, carbamylated BMA; −1°, native BMA; −2°, native BMA. ω = 52 640; CsCl; 25°C; single-sector Kel−F centerpieces; An−F rotor [10].

of the isoconcentration position, r_e, in the gradient column [11]. If the protein banded relatively close (within a millimeter) to r_e, evaluation of $(d\rho/dr)_{r_e}$ (the density gradient at r_e) from published density gradient proportionality constants [12] was sufficient to establish the value of ρ_0, the buoyant density of the protein.

This method suffers to some extent in that it is not an in-the-cell measurement. DNA chemists have used *E. coli* DNA for an in-the-cell marker [13]. Given the assigned density of $\rho_0 = 1.7100$ g/ml for this DNA, the density of a new DNA can be readily obtained from the known density gradient and the distance between the bands.

$$\rho_2 = \rho_1 + \int_{r_1}^{r_2} (\omega^2 r/\beta_B)\, dr . \qquad (1)$$

The densities ρ_1 and ρ_2 are the respective buoyant densities of the two DNAs which band at the radial positions r_1 and r_2, respectively. The value of β_B, the density gradient proportionality constant, can be assumed to be a constant for small values of $(r_2 - r_1)$. This is due in large part to the zero slope of the compositional density gradient at $\rho \approx 1.7$ g/ml. Values of β_B have been tabulated for nucleic acids for three salts [14].

These β_B values cannot be used in protein experiments, even if a marker can be obtained, because they apply solely to nucleic acids and to a much higher density. Values of compositional density gradients, β_0, are available for a wide variety of 1:1 salts [12] and can be used with considerable accuracy if the protein is banded sufficiently close to the marker.

A serious problem arises in the selection of a marker because of the large standard deviation of soluble protein bands. The schlieren patterns of two protein bands would be hopelessly distorted if the bands were formed near each other as required for the use of β^0 values. An alternative occurred to us which has a narrow, non-interfering schlieren image. This is the use of density marker beads produced by Reproductive Systems, Inc. These beads are available in about 1 mm diameters and cover the density range 1.1−1.9 g/ml, in increments of 0.1 g/ml. We have made a number of preliminary tests with these beads in density gradients [15].

Fig. 4 displays the image of one of these beads in a CsCl gradient. It is apparent that the band is sharp enough to permit the accurate determination of a nearby protein band if the density of the bead is known with sufficient accuracy. This has posed the most serious problem for us in developing this method.

A rather considerable variation in the density of individual beads has been observed in CsCl gradients. Thus each bead must be individually calibrated. Initial attempts to calibrate the beads in a CsCl column in the centrifuge were unsuccessful because the beads were found to physically deteriorate after about 2 or 3 runs.

An alternate method of calibration was sought and the Linderstrøm−Lang technique [16−18] was chosen as being simple and yet accurate. The 1-G density gradient apparatus described in Lang's Carlsberg papers was constructed and bromobenzene and benzene employed to establish the density gradient. Several drops

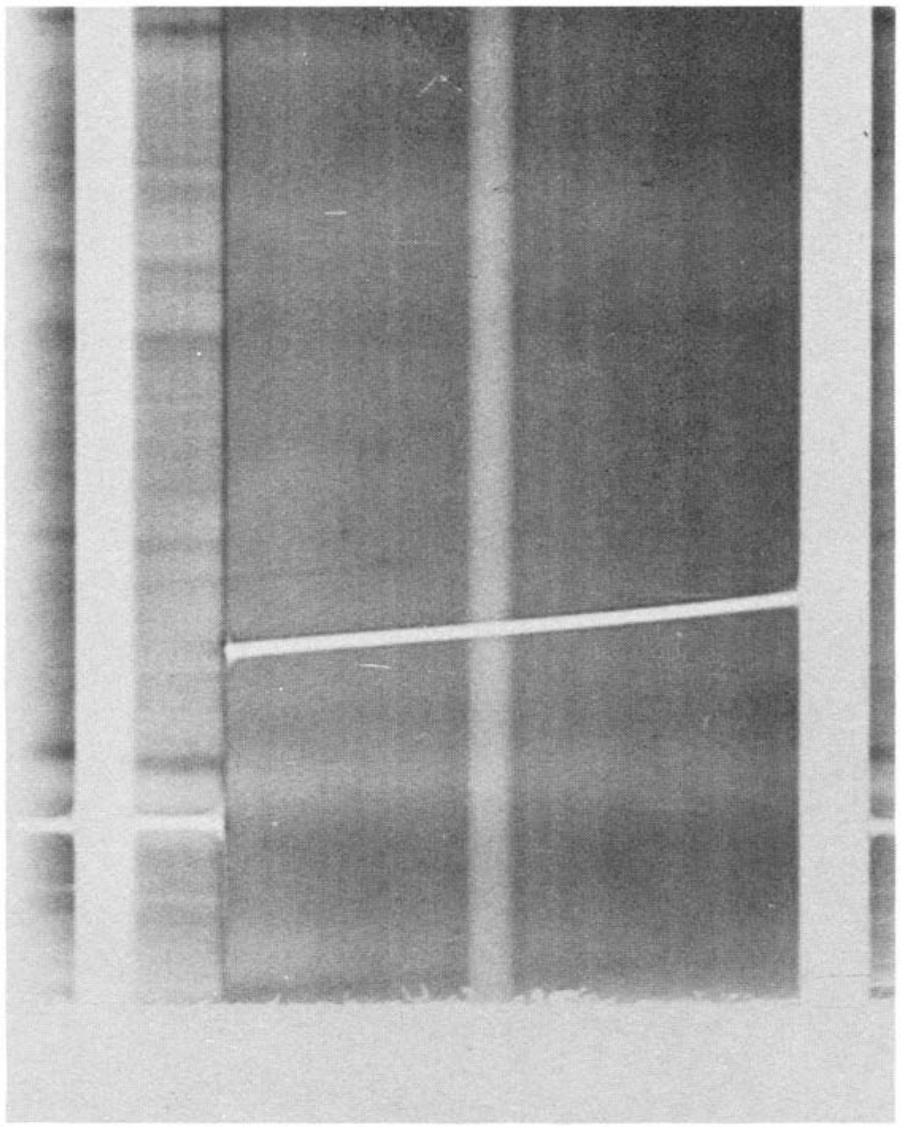

Fig. 4. Equilibrium schlieren photograph of a density marker bead banded in a CsCl gradient of ρ_e = 1.33 g/ml at 56 100 rpm and 25°C. Single-sector, 4°, Kel–F centerpiece [15].

Table 1
Calibration and determination of linearity of a 1-G bromobenzene–benzene density gradient in a Carlsberg column [a]

Drop	$\rho(n_D^{25})$	$\Delta\rho(n, n+1)$	$\Delta x(n, n+1)$	$\Delta\rho/\Delta x$
1	1.239			
		0.029	5.602	0.0051_8
2	1.268			
		0.034	6.540	0.0052_0
3	1.302			
		0.024	4.625	0.0051_9
4	1.326			

[a] Data are from ref. [15].

of CsCl whose densities were established refractometrically were inserted into the column along with several marker beads. The droplet and bead positions were accurately established by means of a travelling microscope. The data in table 1 indicate the column indeed was quite linear and that accurate values for the densities of the beads can be measured with this column.

After calibration, each bead was carefully isolated and its density noted. They were then inserted into regular banding experiments and employed in the calculation of ρ_0. The buoyant densities measured from the marker beads were found to be identical to the ρ_0 value obtained in the usual way from n_D^{25} data, within ± 0.001 g/ml, the limit of accuracy of the refractometric method.

A number of problems remain in our future development of the use of marker beads to determine protein buoyant densities. The pressure dependence of the density of the bead, the possibility of solute binding to the beads, and the use of more accurate density reference solutions (such as KCl solutions) must be investigated before this technique can find widespread usefulness.

2.3. Effect of pressure on the buoyant density of proteins

Hearst et al. [19] reported in an early study on the effect of pressure on the buoyant density of T-4 bacteriophage DNA and tobacco mosaic virus, strain U1. They found that the buoyant density, ρ_0^0, varied linearly with pressure as:

$$\rho_0^0 = \frac{1}{\bar{v}_{s,0}^0}(1 - \Psi P_0). \qquad (2)$$

The quantity $1/\bar{v}_{s,0}^0$ is the buoyant density, ρ_0^0, when the band is at atmospheric pressure and Ψ is proportional to the slope of a ρ_0^0 versus pressure, P, plot. The quantity Ψ was found to be a complicated function of the differential compressibilities of solvent and solvated solute and the variation of buoyant density with water activity.

These authors showed that an effective density gradient must be employed to compute correct values of solvated molecular weights. The expression for this gradient:

$$(d\rho/dr)_{eff} = [1/\beta^0 + \Psi(\rho_0^0)^2](1-\alpha)\omega^2 r \qquad (3)$$

involves Ψ. Therefore values of Ψ must be known, according to this method, before accurate molecular weights can be determined from density gradient experiments.

Subsequent to this, Hearst and Schmid [14] have demonstrated a superior method of obtaining accurate molecular weights. The method consists of banding

two samples of DNA labelled with different density markers in the same CsCl gradient. The difference between the peaks, Δr, the buoyant density, ρ_0, and the average of the two banding positions, r_0, are then measured. These data, combined with the change in mass per nucleotide residue, Δm, and the mass of DNA per cesium nucleotide, yield a quantity directly proportional to the effective density gradient, β_{eff}:

$$G = \frac{1 + \Gamma'}{\beta_{\text{eff}}} = \frac{\Delta m \rho_0}{m \Delta r \omega^2 r_0}. \quad (4)$$

This method suffers from two drawbacks in its application to protein studies. As discussed above, the large standard deviations of protein bands cause considerable difficulty in the overlap of the schlieren patterns. Secondly, it is somewhat more difficult to obtain density labelled proteins than nucleic acids, especially for the mammalian proteins which have been the most widely studied proteins in density gradients to date.

Thus it seemed useful to us to extend these pressure measurements to the field of proteins as Vinograd and coworkers [20] have done for several nucleic acids. Because of the long column length required to encompass an entire protein band, it was not possible to use the variation of oil column length technique employed previously [19]. Instead, speed variation was employed to vary the pressure. An An–H titanium rotor provided angular velocities ranging from 52 640 rpm to 67 770 rpm. The difference in density between ρ_e and ρ_0 was obtained as before [19] and plotted against the hydrostatic pressure at band center. The results are shown in table 2 [21].

These results are interesting in that the Ψ values for BMA are much lower than those obtained previously for several DNAs and the Ψ values for ovalbumin are negative. The latter finding indicates that either the compressibility of the solvated polymer is greater than the compressibility of the solution or that $(\partial\rho_0^0/\partial a_1^0)_P(da_1^0/d\rho^0) > 1$. This is the first observation of a positive slope for a ρ_0^0 vs. P plot.

Table 2
Effect of pressure on the buoyant properties of proteins [a]

Protein	Experiment	$\Psi \times 10^6$ (atm^{-1})
Bovine serum mercaptalbumin	1	11.1
	2	14.1
Ovalbumin	1	−18.3
	2	−2.8

[a] Data are from ref. [21].

2.4. Effect of pressure on buffer pH

Professor Kauzmann of Princeton University has brought to our attention a problem regarding the pH at which centrifuge runs are conducted [22]. Because of the large volume change which occurs upon ionization, the equilibrium between the two forms of the buffer will be significantly altered by the pressure generated in the cell at equilibrium.

The thermodynamic dependence of the equilibrium constant, K, on pressure is given by

$$\frac{d \ln K}{dP} = -\frac{\Delta V}{RT}, \quad (5)$$

where ΔV is the volume change on ionization in ml/mole. If ΔV is independent of pressure:

$$pK_P - pK_1 \doteq \frac{P \Delta V}{2.3RT}. \quad (6)$$

The commonly employed acetic acid–acetate ion buffer system has a ΔV of about 10.0 ml/mole in a 3M salt solution. Insertion of this value into eq. (6) along with P = 185 atom, the pressure at the center of a salt column of ρ_e = 1.3 at 59 780 rpm, yields a pH of 4.724 in contrast to the bench-top pH of 4.757. The depression of the pH by 0.033 unit will not seriously affect most runs. However, the use of amine buffer systems should be avoided because the volume change on ionization is 30 ml/mole which alters the solution pH by 0.10 unit. This effect could be appreciable in some particularly precise work or in the case of a buoyant titration experiment conducted at a pH near an inflection point. Phosphate, carbonate and glycine buffers would display intermediate effects.

It is apparent from this viewpoint that consideration should be given to the magnitude of the volume change upon ionization when buffers are selected for ultracentrifuge work. (See the paper by Dr. Kegeles in this volume for additional discussion of pressure effects.)

2.5. Other features of current operating procedures

A number of changes in the methods by which density gradient runs are conducted and analyzed have occurred since the first work with this method. These are briefly summarized in this section.

2.5.1. Use of the slope of $\beta(\rho)$ plot

It has been shown [11] that the isoconcentration position, r_e, can be determined from the slope of the β vs. ρ plot, which we designate as g, as opposed to the use of published normalized isoconcentration ratios. We have found the use of the g values to have wider applicability and now routinely determine r_e from the relation:

$$(r'_e)^2 - (r_e)^2 = (g\omega^2/\beta_e^2)(r_b^2 - r_a^2)^2/48 , \qquad (7)$$

where r'_e is the root-mean-square position of the top and bottom of the solution column, r_a and r_b, respectively.

2.5.2. Quadratic relations for $n_D^{25}(\rho)$

Quadratic relationships between refractive index, n_D^{25}, and solution density, ρ^{25}, have been obtained for five salts [12]. The most widely used relation is that for CsCl which is:

$$\rho^{25} = 1.1584 - 10.2219(n_D^{25}) + 7.5806(n_D^{25})^2 . \qquad (8)$$

This relation is valid throughout the entire solubility range and should be used in the refractometric determination of densities of CsCl solutions.

2.5.3. Compositional density gradient proportionality constants

Values of β^0 have been computed for 20 1:1 electrolytes [12] so that a wide variety of cations and anions can be selected for the buoyant medium to determine ion-binding effects. Extensive measurements in the centrifuge verified these calculations.

2.5.4. Maximum angular velocities

Care must be exercised in the use of the schlieren optical system that light is not lost due to gradients of refractive index which are too large. It has been found [12] that light will be lost from the optical system if $\omega^2/\beta_e \times 10^2$ exceeds the following values: 1.85 ± 0.21 for $+1^\circ$ windows, 2.42 ± 0.08 for flat windows, and 3.45 ± 0.35 for -1° windows. Thus, the angular velocity must be selected with some caution for salts with relatively small β values in order that a portion of the image is not lost.

2.5.5. Plate measurement

We currently measure all radial distances except r_0 with the micrometer heads of a Nikon 6C microcomparator. The band center is determined by tracing the schlieren pattern onto vellum paper directly from the projected image of the comparator and interpolation of the baseline.

3. Results for proteins and polypeptides in buoyant salt solutions

Our laboratory has been active for the past six years in the measurement of the buoyant densities of a variety of proteins and polypeptides over a wide range of pH in several different buoyant media. The following sections provide an overview of the work we have published and work in progress in this area.

3.1. Buoyant densities of proteins at the isoelectric point in CsCl

The technique of density gradient centrifugation has been widely employed to measure the buoyant densities of a large number of cesium DNAs. The current edition of the Handbook of Biochemistry, Selected Data for Molecular Biology [23] lists the buoyant densities for over 300 different DNAs but no data for proteins. Because the buoyant density is an intrinsic property of each protein, it seemed reasonable to us to measure the ρ_0 values of a large number and variety of proteins. The proteins studied were selected on the basis of having molecular weights greater than 10 000 g/mole so that the standard deviations would not be too large, having known partial specific volumes in order that hydrations could be computed, and having the percentage of prosthetic groups less than a few per cent so that the buoyant densities would primarily reflect the amino acid composition.

Table 3 provides the data for the proteins which have been measured to date [24]. The buoyant densities at the isoelectric point for 24 proteins have been determined. They range from 1.25 g/ml to 1.37 g/ml. This is in distinct contrast to the nucleic acids which

Table 3
Buoyant densities and net hydrations of proteins in CsCl solutions at the isoelectric point at 25°C [a]

Protein	pH	ρ_0 (g/ml)	Γ' (g H_2O /g protein)
Hemoglobin (human)	7.04	1.250	0.26
Myoglobin (whale)	6.72	1.256	0.27
Hemoglobin (horse)	6.55	1.264	0.20
Hemoglobin (pig)	6.58	1.272	0.17
β-lactoglobulin	5.39	1.272	0.16
Aldolase (rabbit muscle)	6.56	1.273	0.20
Hemoglobin (dog)	–	1.274	0.17
Bovine serum mercaptalbumin	5.50	1.282	0.20
Histone (calf thymus)	9.12	1.284	0.18
Ovalbumin	4.71	1.284	0.14
Cytochrome C (horse heart)	7.91	1.289	0.31
Chymotrypsinogen A	9.45	1.293	0.23
Catalase	5.48	1.299	0.17
7S Immuno gamma globulin	7.30	1.300	0.13
Conalbumin	6.28	1.306	0.14
Ribonuclease	10.55	1.306	0.25
Concanavalin A	8.07	1.308	0.15
α-chymotrypsin	8.65	1.310	0.12
Trypsinogen	9.11	1.312	0.11
Lysozyme (chicken)	10.50	1.319	0.23
Carboxypeptidase	6.72	1.319	0.16
Pepsin	0.76	1.319	0.035
Edestin	5.62	1.328	0.037
Pepsinogen	3.79	1.332	0.003
Hemocyanin	5.17	1.339	0.030
Gliadin	5.91	1.366	0.030

[a] Data are from ref. [24].

have densities of about 1.70 g/ml for DNA and even higher for RNA.

The net hydrations were computed from the standard relation [25]

$$\rho_0 = \frac{1 + \Gamma'}{\bar{v}_3 + \Gamma'\bar{v}_1}. \qquad (9)$$

These hydrations vary between 0.03 g H_2O/g protein and 0.31 g H_2O/g protein, in reasonable agreement with a variety of other techniques. Kuntz and Kauzmann [26] have recently reviewed these data and compared them with hydration values obtained by a variety of other techniques.

The buoyant density of a polymer should reflect to at least a good first approximation its monomer composition. Thus an ancillary goal of this work is to provide a correlation between buoyant and amino acid

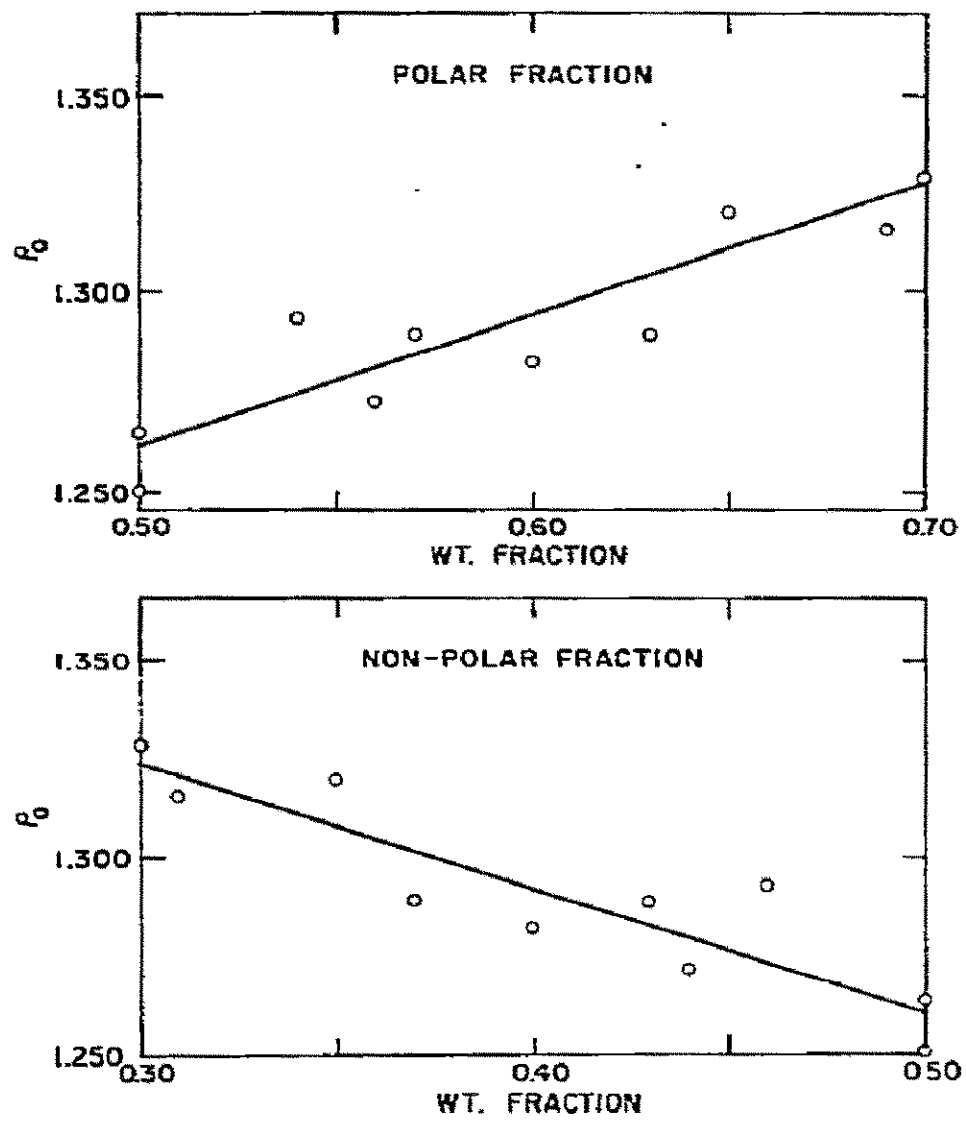

Fig. 5. The buoyant densities of proteins in CsCl at 25°C as a function of the weight fraction of polar and non-polar residues [24].

composition. Residues have been grouped as ionic, non-ionic, polar, acidic, and basic. Plots of ρ_0 versus the weight or mole fraction of each of these variables have shown that the best correlation is obtained for buoyant density versus the weight fraction of polar and non-polar groups. These data are given in fig. 5.

The data demonstrate that no simple relationship can be expected as in the G–C contents of DNAs. It appears as of now that variations in prosthetic groups, hydration, and ion-binding are sufficient to preclude a linear relationship.

3.2. Buoyant titrations of proteins in CsCl

The variation of buoyant density with pH is of interest because as groups are deprotonated, the charge on the protein varies and this should be reflected in changes in hydration and/or ion-binding which in turn should alter the buoyant density. We have measured the complete buoyant titrations of three proteins and

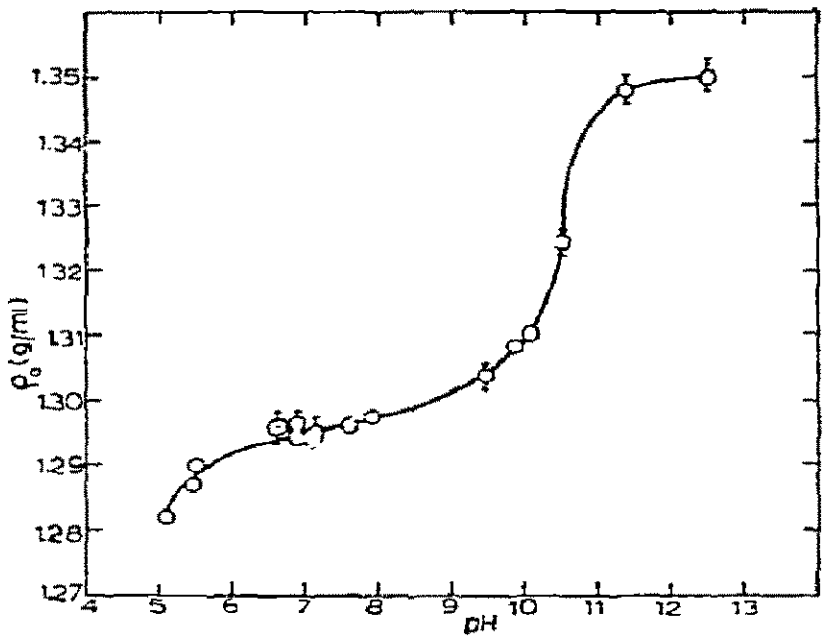

Fig. 6. Buoyant density, ρ_0, of bovine serum mercaptalbumin in CsCl as a function of pH. All runs performed in 4°, single-sector. Kel–F centerpiece at 56 100 rpm and 25°C. Diameters of circles or error flags represent maximum experimental uncertainties [27].

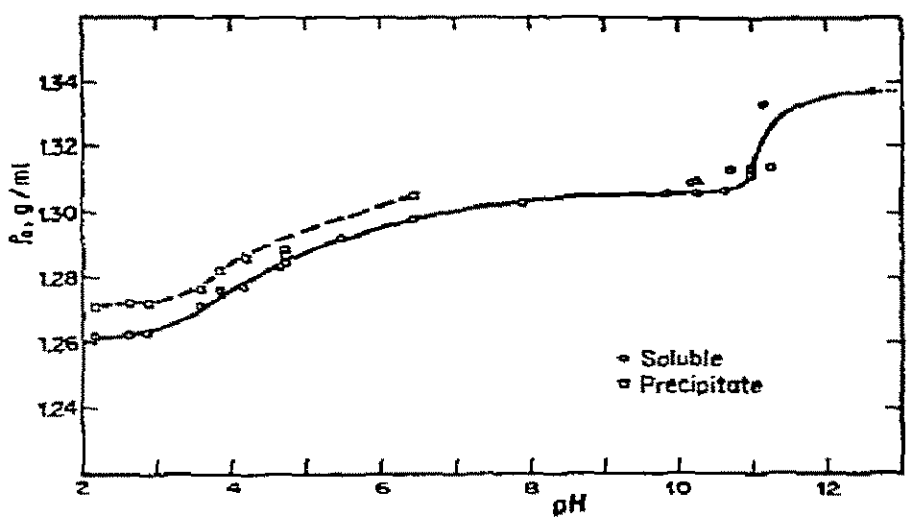

Fig. 7. Buoyant densities of soluble and precipitated ovalbumin as a function of pH; CsCl; 25°C [22].

partially complete data are available for three others. These data require between 10 and 15 separate density gradient experiments for each titration in CsCl solutions buffered by between 0.01–0.03 M buffers of the desired pH.

3.2.1. Results

These six titration curves are presented in figs. 6 through 9.

Williams and Ifft [27] reported the first protein buoyant titration. Fig. 6 shows these data for bovine serum mercaptalbumin, BMA, as they extend from pH 5 to 12.5. The precision of their measurements is

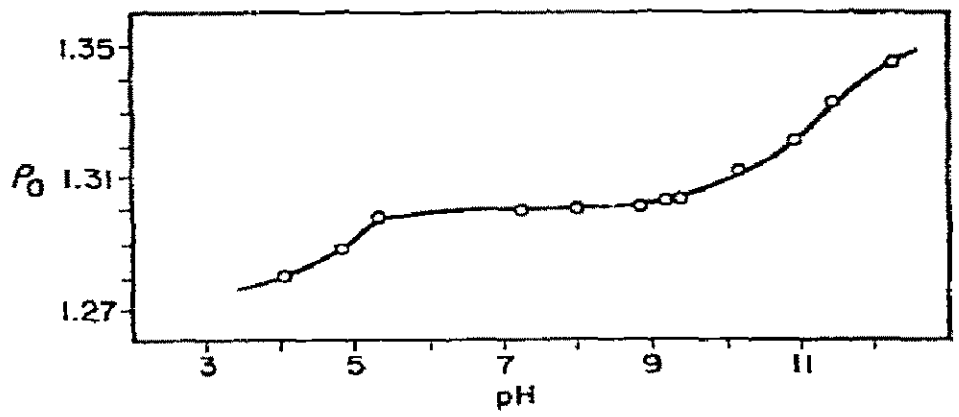

Fig. 8. Buoyant density of human immuno-gamma globulin as a function of pH; CsCl; 25°C [29].

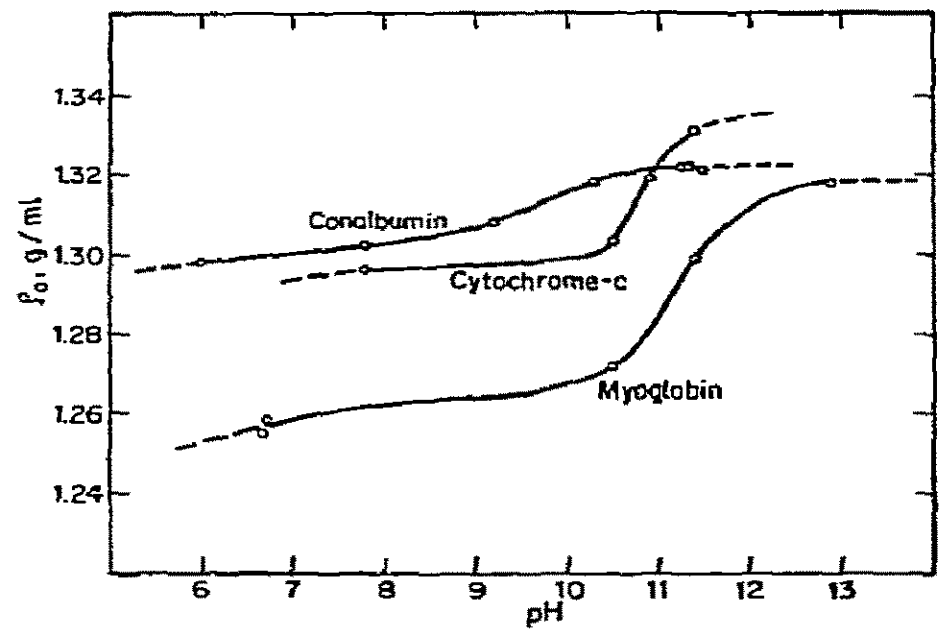

Fig. 9. Buoyant densities of conalbumin, cytochrome-C, and myoglobin as a function of pH; CsCl; 25°C [30].

reflected in the size of the data circles. This curve has recently been extended to pH 2 by a visitor to this laboratory, Dr. Ib Svendsen, Assistant Director of the Carlsberg Laboratorium, Copenhagen, Denmark [28].

The buoyant titration curve of ovalbumin [22] covered the entire range from pH 2 to 12. At pH's below 6, the protein samples contain both soluble and precipitated material. In many cases, the buoyant densities of both forms of the protein can simultaneously be measured. Fig. 10 is an example of this behavior. The narrow band of precipitate causes the light loss just to the right of band center. In general, we have found that the density of the aggregated protein is about 0.006–0.009 g/ml more dense than the soluble form.

The data in fig. 8 were obtained for a pooled sample

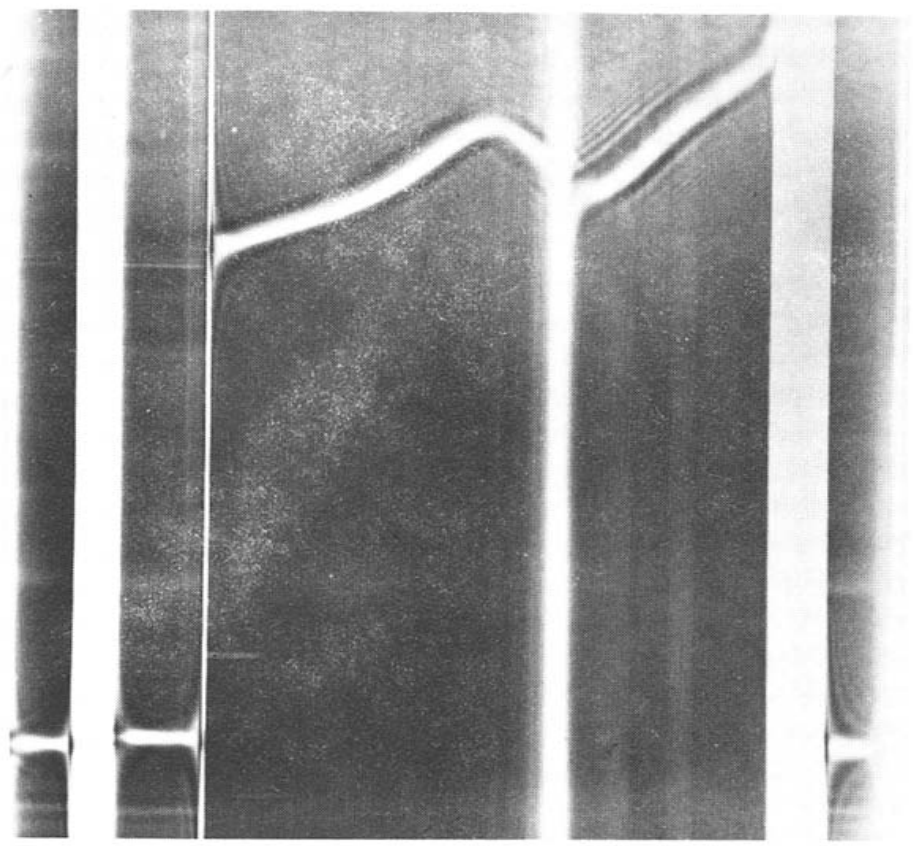

Fig. 10. Equilibrium schlieren photograph of 0.1% ovalbumin in CsCl of ρ_e = 1.278 g/ml, pH = 4.66, acetate buffer (μ = 0.01) at 56 100 rpm and 25° C. Single sector, 4°, Kel–F centerpiece [22].

of human immuno-gamma globulin [29]. Data cannot be obtained for a greater pH range for this material because of molecular stability problems. Fig. 9 gives partially complete curves for the three proteins, conalbumin, cytochrome-C and myoglobin [30].

3.2.2. Discussion

An attempt has been made to fully interpret these curves in terms of hydration and ion-binding only in the case of BMA [27]. This is because ion-binding data are available for BMA at its isoelectric point [31]. BMA binds 53 chloride ions in a 3 M CsCl solution which corresponds to a buoyant composition. Because of electroneutrality and because the protein is at its pI, it is assumed that 53 cesium ions are concomitantly bound in a secondary layer. Therefore, the total hydration of the protein salt complex, Γ'_*, can be computed from the following equation:

$$\rho_0 = \frac{1 + \nu_{Cs^+}\frac{M_{Cs^+}}{M_3} + \nu_{Cl^-}\frac{M_{Cl^-}}{M_3} + \Gamma'_*}{\bar{\upsilon}_3 + \nu_{Cs^+}\frac{M_{Cs^+}}{M_3}\frac{\bar{V}_{Cs^+}}{M_{Cs^+}} + \nu_{Cl^-}\frac{M_{Cl^-}}{M_3}\frac{\bar{V}_{Cl^-}}{M_{Cl^-}} + \Gamma'_*\bar{\upsilon}_1} \quad (10)$$

This equation was employed in the above calculations on an intuitive basis. It has recently been derived thermodynamically [32]. Γ'_* was found to be 0.45 g/ml.

Similarly, the value of Γ'_* was obtained at pH 12.5 with the assumption that the molecule was fully deprotonated. Its value there was 0.48 g/ml. Because of this small variation over a wide pH range, Γ'_* was assumed to vary linearly throughout the range of the buoyant titration.

Therefore, values of ρ_0, $\bar{\upsilon}_3$, the partial specific volume of the protein, $\bar{V}_{Cs^+}$ and $\bar{V}_{Cl^-}$ the partial molar volumes of these ions, and Γ'_* were available at all pH's for use in eq. (10). However, a second relation involving ν_{Cs^+} and ν_{Cl^-} the number of ions bound per BMA molecule, was needed to complete the calculation. The conservation of charge relation, $\nu_{Cs^+} = \nu_{Cl^-} - \phi$, was employed where ϕ is the algebraic charge on the protein. This charge was computed from the published values of pK_{int} by Decker and Foster [33].

The values obtained for ν_{Cs^+} and ν_{Cl^-} as a function of pH by the combination of these two equations are given in fig. 11. Large increases in Cs^+ binding are noted in the pH range where the tyrosines titrate and decreases in ν_{Cl^-} are observed where the lysines are deprotonated. These data were employed to calculate classes of binding sites and to estimate the numbers of ions bound to specific residues.

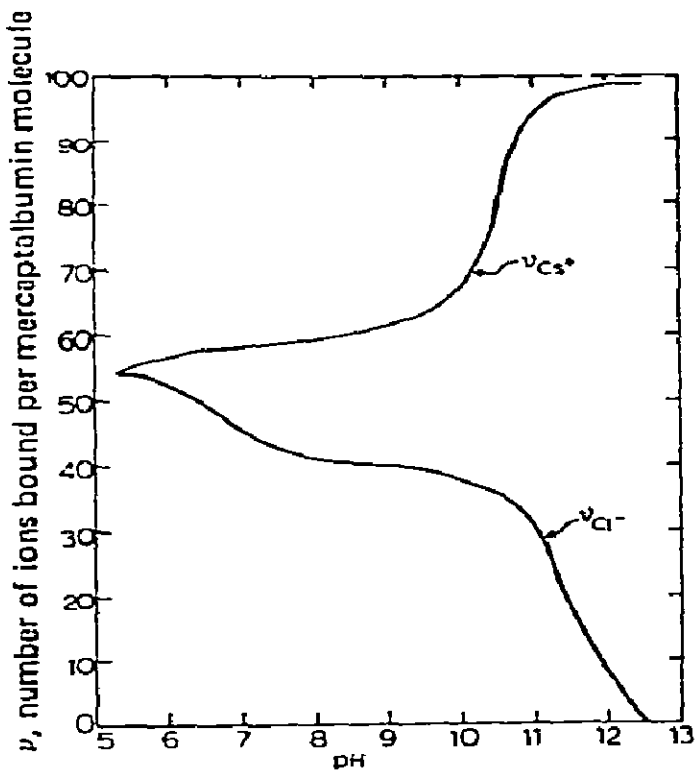

Fig. 11. The number of cesium and chloride ions bound per molecule of BMA as a function of pH; CsCl; 25° C [27].

Similar computations are not possible for the other five proteins because independent ion-binding data are not available at any pH. The following more general types of observation are possible in these cases.

The general shapes of all protein buoyant titrations obtained to date are the same. The shape of the titration curve of the glycoprotein, ovalbumin, of molecular weight 45 000 daltons is quite similar to the titration curve of human IgG of molecular weight 153 000 daltons.

The curves which extend down to pH 2 or 3 exhibit modest inflections at about pH 4.5. This corresponds to the pK's of the glutamic and aspartic residues. Relatively small density changes are observed in the mid pH range of 6 to 9. This is in agreement with the small numbers of histidines normally found in proteins. Large inflections are observed for all six proteins at high pH. The inflection pH of 10.8 ± 0.3 which is displayed by 5 of the proteins corresponds to the expected titration of the lysine and tyrosine residues. The inflection pH of 9.5 for conalbumin suggests the presence of abnormal lysines and/or tyrosines.

Two factors contribute to these density increments. As the pH increases, the net charge on the protein becomes more negative. This must be compensated for by a loss of chloride ions or a gain of cesium ions. Because there is an increase in density in every case, the leaving chloride ions must be heavily hydrated such that their density is less than that of the protein. The expected density of a cesium ion in a CsCl solution of density 1.3 g/ml is 6.7 g/ml [34]. Calculations for the ovalbumin titration curve [22] show that the low pH density increment must be due to a loss of Cl^- and not a gain of Cs^+. At high pH, the increase in density for both ovalbumin and BMA has been shown to be primarily due to a gain of Cs^+.

The second factor causing these density increments is the volume changes of the titrating groups themselves. It can be shown [22] that the density change, $\Delta\rho$, to be expected for a species of density, ρ, and volume, v, which undergoes a volume change, Δv, is:

$$\Delta\rho = -\rho\Delta v/v\,. \qquad (11)$$

This density change accounts for 0.021 g/ml out of the total change of 0.033 g/ml which ovalbumin exhibits at low pH. At high pH, the change in density which is expected due to volume changes caused by the lysine deprotonation alone is −0.011 g/ml. Thus this $\Delta\rho$ must be added to the observed density change of 0.018 g/ml to give the $\Delta\rho$ due to ion-binding effects.

Another way to interpret these titration curves is to look for correlations between density changes at the inflection pH's and amino acid compositions. A plot of $\Delta\rho$ versus mole fraction of the ionizable lysine and tyrosine residues yielded a straight line which passed through the origin for three of the five proteins studied. Difficulties in determining the actual numbers of lysines and tyrosines which titrate with normal pK's preclude an extension of these studies at present.

As discussed above, hydration values, Γ', can be computed at pI for each of these proteins. If ion-binding effects are neglected and it is assumed that $\bar{v}_3$ does not change with pH, Γ' values can be computed for all ρ_0's throughout the pH range studied. As in the case of BMA, Γ'_* values can be obtained at the extremes of pH if assumptions are made about the ionic composition of the species. Computations for ovalbumin reveal values of 0.23 g H_2O/g protein at pH 2 and 0.41 g H_2O/g protein at pH 12. This variation in Γ'_* with pH is in distinct contrast to the observations discussed above for BMA.

3.3. Buoyant titrations of synthetic polypeptides

It is apparent that the interpretation of the buoyant titrations of proteins is quite difficult due to the 20 different amino acids, the number, state and availability of charged and polar residues which influence the hydration and ion-binding of proteins and a variety of complicating structural features. It seemed apparent a few years ago that it would be most helpful to do parallel buoyant titrations for a number of homo- and copolypeptides. Such measurements should provide information as to the values of ρ_0 of each residue in its fully protonated and fully deprotonated forms, the magnitude of $\Delta\rho$ upon ionization, whether or not there are any buoyant density changes when no ionization occurs, and the inflection pH's. A number of these measurements have been completed and they have been helpful in understanding the behavior of proteins.

3.3.1. Buoyant titrations of ionizable homopolypeptides in CsCl

The buoyant titrations of six ionizable homopoly-

peptides have been measured in CsCl solutions [35]. The results are given in fig. 12. A number of general observations can be made from these curves.

The buoyant densities of all residues increase with increasing pH. This parallels the observation for all proteins measured to date. In each case, an inflection pH can be noted which occurs near the pK of that amino acid side chain. The buoyant densities of these residues do not vary unless the residue is titrating. As indicated on the figure, all of the homopolypeptides are soluble in CsCl solutions of buoyant composition in the charged form but all are insoluble in the neutral form. This figure graphically displays two classes of peptides, those with inflections at pH 5 and those near pH 10. The unusual inflection pH for poly(Arg) will be discussed later.

The explanations of these observations are similar to those advanced earlier for proteins. As the pH is increased, eventually the pK_{int} value is reached, deprotonation occurs and a combination of the volume change upon ionization and ion-binding changes leads to density increments. It is assumed that Cs^+ binding occurs upon deprotonation of the glutamic acid and tyrosine residues and the loss of heavily hydrated

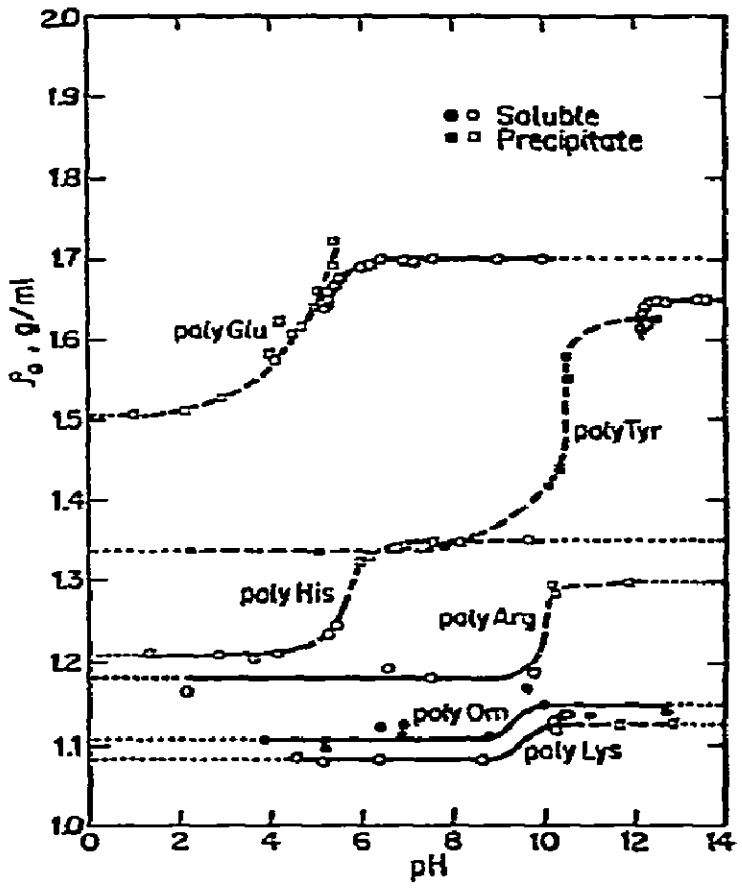

Fig. 12. Buoyant densities of six ionizable homopolypeptides as a function of pH; CsCl; 25°C [35].

Table 4
Buoyant densities of homopolypeptides in CsCl at 25°C [a]

Homopolypeptide	Buoyant densities, ρ_0		$\Delta\rho_0$
	Low pH	High pH	
poly(Lys)	1.084	1.122	0.038
poly(Orn)	1.111	1.134	0.023
poly(Arg)	1.177	1.297	0.120
poly(His)	1.210	1.350	0.140
poly(Tyr)	1.339	1.651	0.312
poly(Glu)	1.505	1.700	0.195

[a] Data are from ref. [35].

chloride ions (of density less than the residue itself) occurs upon neutralization of the four basic residues.

The actual values of the buoyant densities of these six homopolypeptides at pH's below and above the inflection regions are given in table 4. The densities range from a low value of 1.084 g/ml for poly(Lys) to a high value of 1.700 g/ml for poly(Glu). The fact that the buoyant densities of all proteins observed to date fall in the 1.25–1.37 g/ml range indicates that the amino acids are reasonably uniformly represented in these 24 proteins. The buoyant densities are roughly inversely dependent on side chain length. The side chains of lysine, ornithine and arginine consist of three or four carbon atom chains which end in an ionizable nitrogen atom. These polymers have the lowest density. Poly (Glu) which has the shortest side chain has the largest density. The cyclic residues have intermediate densities.

Preferential hydrations for each residue were computed from the buoyant density of the neutral form and partial specific volumes of the polypeptide determined from the methods and data of Cohn and Edsall [36]. Values of Γ' are given in table 5. A large range from practically no hydration for poly(Glu) up to the high value of 0.89 g H_2O/g polypeptide is observed. Values of Γ'_* are also given in table 5 for the ionized or charged form of the polypeptides. These values are much larger than the Γ' values because thev reveal additional water which is bound to the polymer in order to provide a buoyant composition for the Cs^+ and Cl^- ions which are assumed to be bound to the charged residues.

The buoyant titration of poly(Orn) was measured in an effort to assess the effect of one methylene group in the side chain of a polypeptide on the buoyant

Table 5
Preferential hydrations of neutral homopolypeptides, Γ', and homopolypeptide-ion complexes, Γ'_*, in CsCl at 25°C [a]

Homopolypeptide	$\bar{v}_3$ (ml/g)	Γ' (g H_2O/g polypeptide)	Γ'_* (g H_2O/g polypeptide)
poly(Glu)	0.661	0.01	0.91
poly(Tyr)	0.712	0.14	0.66
poly(His)	0.665	0.29	1.16
poly(Arg)	0.694	0.34	1.31
poly(Orn)	0.777	0.89	1.99
poly(Lys)	0.819	0.70	2.31

[a] Data are from ref. [35].

density. This was done by measuring the buoyant titrations of poly(Orn) and poly(Lys) which differ by just one $-CH_2-$ group. The entire poly(Orn) curve was then predicted from the poly(Lys) curve using the assumptions of additive volumes and a density of a methylene group of 0.859 g/ml as employed in a number of organic chemistry applications. The success of this prediction suggests that the titration curves of other homologues, such as poly(Asp), may be predicted from the data for poly(Glu).

These data have been successfully employed to predict the low pH behavior of several proteins. The expected density increment at low pH for a protein should be the increment observed for poly(Glu) (0.195 g/ml) times the mole fraction of ionizable carboxyl residues in the protein. These calculations yield values of 0.026 g/ml and 0.023 g/ml for ovalbumin and human IgC respectively. The good agreement of these values with the observed $\Delta\rho$'s for these two proteins, 0.033 g/ml and 0.021 g/ml, suggests that most of the carboxyl groups in the protein titrate with normal pK's and that these residues interact with the solvent in about the same way in the protein as in the homopolypeptide. It is apparent that this homopolypeptide data will be useful in predicting and interpreting the behavior of proteins in buoyant titrations.

3.3.2. Buoyant titrations of non-ionizable homopolypeptides in CsCl

The buoyant behavior of the non-ionizable polypeptides was assumed to consist of an insoluble polymer which displayed a pH-independent buoyant density. To assess these assumptions and to determine the magnitude of the buoyant densities of such residues, the buoyant titration curves of poly(Gly) and poly(Ala)

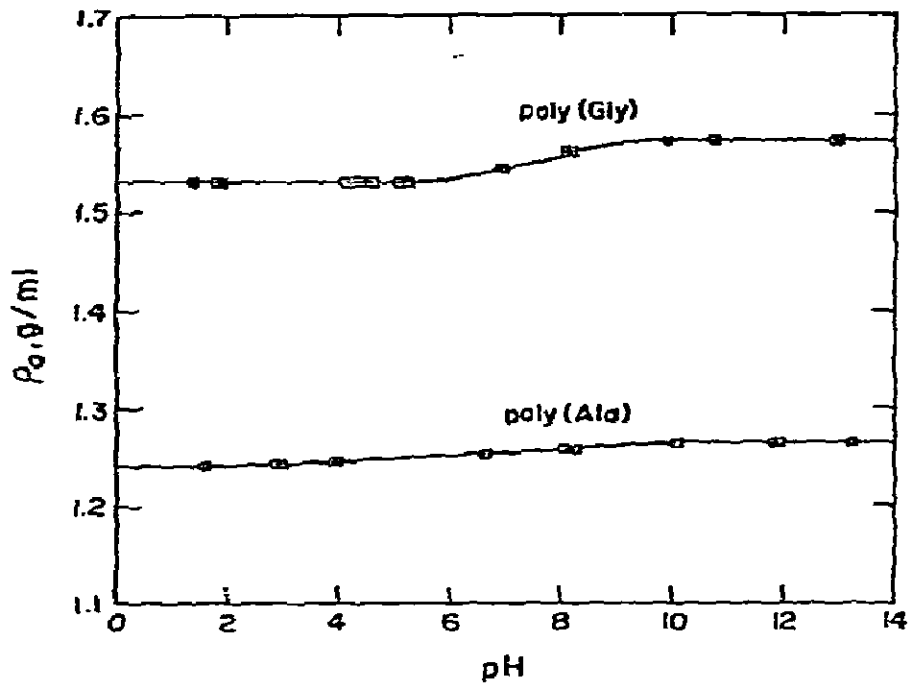

Fig. 13. Buoyant densities of two non-ionizable homopolypeptides as a function of pH; CsCl; 25°C [32].

were measured [32]. The surprising results are shown in fig. 13. Although neither residue contains any ionizable hydrogens, a definite inflection occurs at pH 7–8 in both cases. The inflections are experimentally significant and are of the order of magnitude of those observed for poly(Lys) and poly(Orn).

A possible explanation of this behavior is that the pK's of the α-NH_2 groups of these amino acids are about 8. If the degree of polymerization in each case was rather low, the titration of these end groups could contribute a small inflection $\Delta\rho$. The molecular weight of the poly(Gly) sample was indeterminable but that of the poly(Ala) sample was 2680 daltons/molecule which corresponds to a degree of polymerization of 38. Thus the observed $\Delta\rho$ should have been only about 0.001 g/ml which is much smaller than the observed value. No satisfactory explanation of this phenomenon has been found to date.

3.3.3. Buoyant titrations of copolypeptides in CsCl

As a first step in the utilization of the homopolypeptide data for the prediction of the buoyant titration behavior of proteins, the buoyant titrations of five copolypeptides were measured [32]. The polymers studied were poly(Glu$^{60.9}$)(Lys$^{39.1}$), poly(Glu$^{90.9}$)(Ala$^{9.1}$), poly(Glu$^{93.8}$)(Tyr$^{6.2}$), poly(Glu$^{54.5}$)(Tyr$^{45.5}$), and poly(Lys$^{51.4}$)(Tyr$^{49.6}$). Although the sequences are unknown, the amino acid compositions were measured accurately.

The buoyant titration of the poly(Glu)(Lys) copolymer is displayed in fig. 14. These data are rather typical of all of the copolymers. As expected, the copolymer buoyant densities are intermediate between those of poly(Glu) and poly(Lys) at corresponding pH's. Similarly, inflections are noted for the copolymer at about the same pH's as for the homopolymers.

A variety of methods of calculation were explored to calculate the copolymer data from the homopolypeptide data. The additive volume relationship, eq. (12), is reasonable on physical grounds and can be derived readily. It was used in all computations to compute a predicted buoyant density, ρ_p.

$$\frac{1}{\rho_p} = \frac{W_a}{\rho_a} + \frac{W_b}{\rho_b} \quad . \tag{12}$$

The buoyant densities of the two constituent monomers, ρ_a and ρ_b, are present with weight fractions W_a and W_b in the copolypeptide. The weight fractions reflect the mole fractions of the respective constituents in the copolypeptide, the weights of the amino acid residues, bound water, and bound ions if applicable.

Two methods of calculation were applied to eq. (12). In both methods, one ion of opposite charge was assumed to be bound to the charged form of the polymer. The two methods differ as to how the hydration was calculated. Method A assumes that the Γ' values computed from eq. (9) for the neutral form of the polypeptide were constant for all pH values. This does not appear to be as reasonable physically as method B in which the hydrations for the ion-polypeptide complex were computed as Γ'_* values (eq. (11)). This latter calculation was complicated by the necessity of using an iterative procedure to account for the difference in partial specific volumes of the bound Cs^+ or Cl^- at the different densities of the homo- and copolypeptides.

Fig. 14 indicates that method A is somewhat superior to method B. This was generally found to be the case for the other 4 copolypeptides as well. However, it is apparent from these data that neither method permits precise predictive ability. Perhaps configurational changes or internal ion pairs prevent better agreement than is demonstrated here.

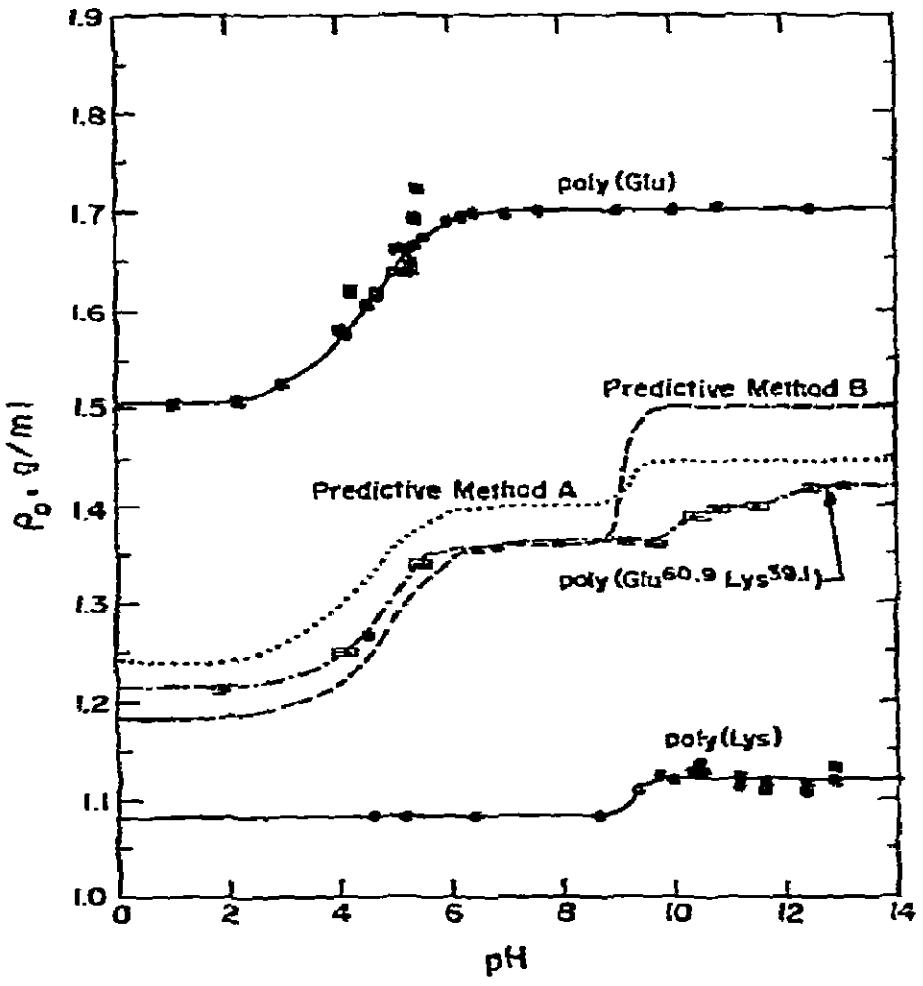

Fig. 14. Measured and predicted buoyant densities of poly (Glu$^{60.9}$) (Lys$^{39.1}$) as a function of *pH*; CsCl; 25°C [32].

3.3.4. Poly(Lys) and poly(His) in several salt gradients

The buoyant behavior of BMA in several buoyant solutions has been measured [6]. For instance, the ρ_0 of BMA was found to increase as 1.282, 1.315 and 1.347 in the anion series of cesium salts; CsCl, CsBr, and CsI. Thus, it was of interest to examine whether a series of salt solutions would display similar effects on the buoyant density of homopolypeptides and also how the buoyant titration curves would be effected. Because of the model of one-to-one ion binding, a cation series would be particularly interesting for the acidic residues and an anion series for the basic residues. However, we were restricted to the study of poly(Lys) and poly(His) because their ρ_0's are low enough to be

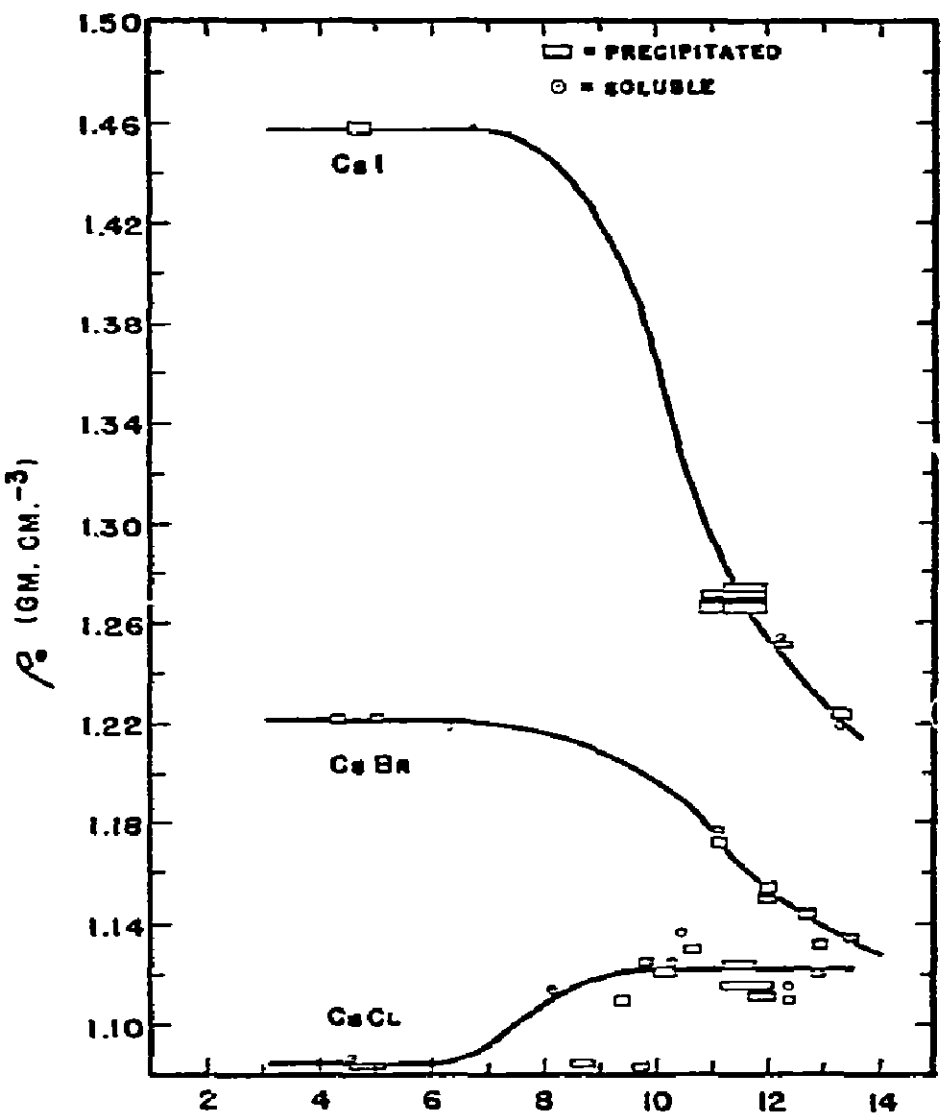

Fig. 15. Buoyant densities of poly(Lys) in three salts as a function of pH; 25°C [37].

banded in a variety of salt solutions which have limited solubilities.

The results for poly(Lys) in CsCl, CsBr and CsI are displayed in fig. 15 [37]. The low pH buoyant densities increase in the same order as for BMA – 1.085, 1.221 and 1.458 – for the Cl^-, Br^-, and I^- series. The larger bound anion or the decreased water activity has a profound effect on the buoyant density. Partial specific volumes of these anions in concentrated salt solutions will have to be computed before this effect is understood.

The titration curves in CsBr and CsI are the first instances observed for any polymer in which the buoyant density decreases with increasing pH. This has not been observed for ΦX-174 DNA [38] or any of the proteins or polypeptides reported in this paper. However, all prior buoyant titrations were measured in CsCl. It would appear that the leaving Br^- and I^- ions are less heavily hydrated than the Cl^- ions.

The three curves extend up to about pH 13.2. They cannot be carried further because of the difficulty in calculating the CsCl–CsOH gradients as well as the possibility of the hydrolysis of the polypeptide. Nevertheless, it is apparent that the curves are converging toward a common value which indicates that water activity is not a dominant factor in determining the buoyant density of the neutral form of poly(Lys).

Table 6 gives the buoyant densities of poly(Lys) and poly(His) at low and high pH for a number of salt solutions. It is apparent from these data that the nature of the cation has little effect on ρ_0, the nature of the anion has a large effect, and the buoyant densities of the neutral, high pH form of the polymer are independent of the banding medium.

3.4. Buoyant titrations of chemically modified proteins

The buoyant titrations discussed earlier in this paper provide information as to inflection pH values and give the density increments associated with deproton-

Table 6
Buoyant densities at low and high pH of poly(Lys) and poly(His) in various salt solutions at 25°C [a]

		Buoyant densities	Buoyan
	Solvent	Low pH	High pH
poly(Lys)	CsCl	1.085	1.120
	CsBr	1.221	1.134
	CsI	1.458	1.224
	RbCl	1.109	1.112
	RbBr	1.265	1.140
	KBr	1.345	1.141
	RbBr	1.265	1.140
	CsBr	1.221	1.134
	RbCl	1.109	1.112
	CsCl	1.085	1.120
poly(His)	CsCl	1.210	1.350
	CsBr	1.442	1.382
	RbCl	1.238	1.359
	RbBr	1.471	1.366
	KBr	– [b]	1.360
	RbBr	1.471	1.366
	CsBr	1.427	1.382
	RbCl	1.238	1.359
	CsCl	1.210	1.350

a) Data are from ref. [37].
b) The ρ_0 of poly(His) at low pH exceeds the solubility of KBr.

ation. However, at high pH, the titration of the lysines and tyrosines occurs concomitantly and it is not possible from a buoyant titration alone to assess the contribution of each class of residues separately. An alternative approach is to selectively modify each residue in turn in such a way as to produce a chemically modified protein having the same structure as the native polymer, but with one class of residues replaced by another group of the same charge, opposite charge or a neutral group. In this way, the contribution of each class of amino acids can be assessed. Three such studies have been completed to date.

3.4.1. Carbamylation of ovalbumin

The technique proposed by Stark [39] and modified by Svendsen [40] was selected as a gentle yet quantitative means to replace the positively charged ϵ-NH_3^+ groups of the lysine residues with a neutral, unsymmetrical urea group:

$$R-(CH_2)_4-NH_3^+ \xrightarrow[pH\ 9.0]{OCN^-} R-(CH_2)_4-NH-\overset{\overset{O}{\|}}{C}-NH_2 \qquad (13)$$

The new group is the residue of homocitrulline. It is stable to acid hydrolysis and thus the extent of modification can be determined quantitatively by standard amino acid analysis techniques. A 17-hour reaction in a pH-stat yielded the modification of 18 out of the 20 lysines of ovalbumin [22].

The buoyant titrations of the native and carbamylated material were measured. The results are given in fig. 16.

The buoyant density of the modified protein is higher than that of the native material at all pH's. In the absence of structural changes, the difference in density between the two curves at high pH, 0.007 g/ml, may be attributed to the 18 new carbamyl groups. This difference was subtracted from the $\Delta\rho$ observed in the mid-pH range, 0.025 g/ml, to give a contribution of 0.018 g/ml by the 18 modified residues. The $\Delta\rho$ observed for poly(Lys) was 0.040 g/ml. Thus, the expected $\Delta\rho$ in ovalbumin would be this value times the mole fraction of lysine residues in ovalbumin or $0.040 \times 18/377 = 0.0018$ g/ml. The factor of ten discrepancy has no explanation at present. However, both the model compound data and the measured contribution of the lysine residues suggest a much smaller contribution to the observed density change than the observed $\Delta\rho$. This plus the inflection observed in the modified titration curve at pH 11.8 indicate that other groups titrate in this region as well. This suggests that the pK of the tyrosines in the ovalbumin molecule in concentrated salt solutions is much lower than the 12.5 value observed for native ovalbumin.

These data were used to demonstrate that the density increment for native ovalbumin at high pH must be due to the combination of the loss of heavily hydrated Cl^- and a gain of Cs^+.

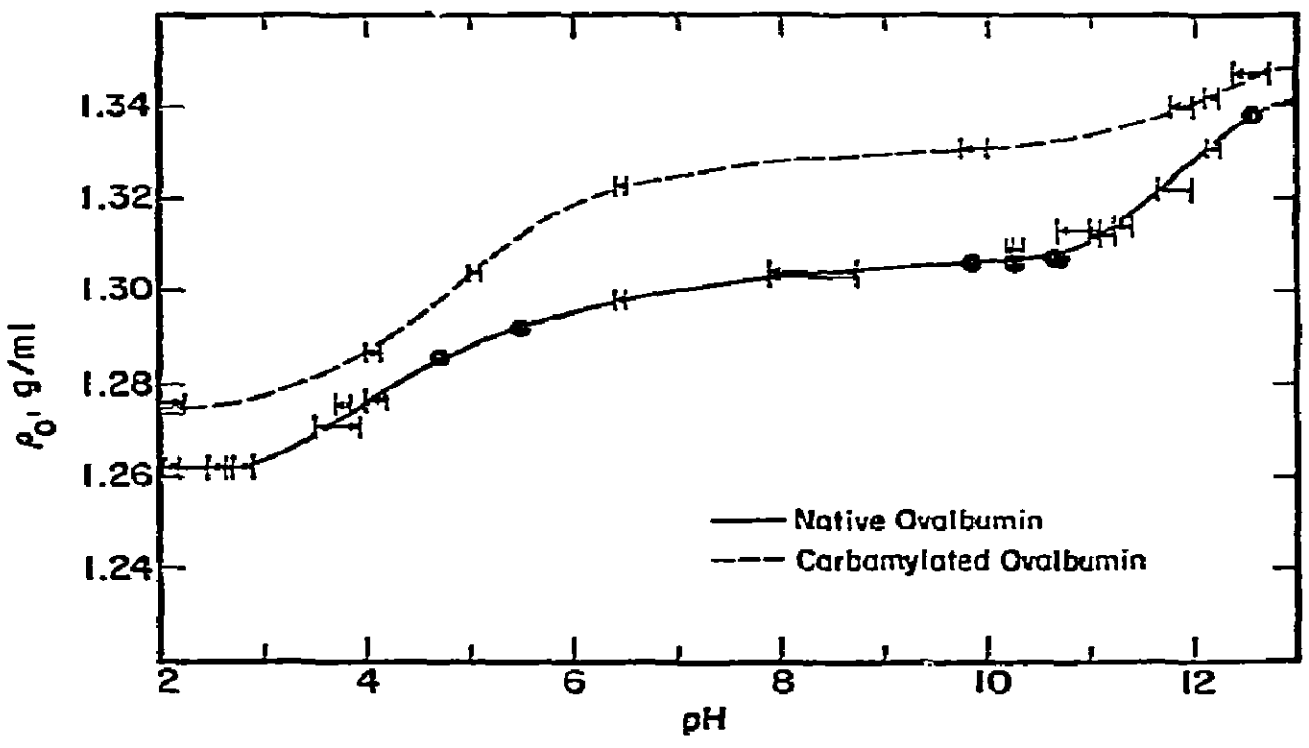

Fig. 16. Buoyant densities of native and carbamylated ovalbumin as a function of pH; CsCl; 25°C. The arrows display the pH shifts with time, $pH_{initial} \rightarrow pH_{final}$. Runs involving no pH shifts are indicated by • [22].

3.4.2. Carbamylation of bovine serum mercaptalbumin

A second study of a carbamylated protein in CsCl gradients was made to determine whether the behavior observed for ovalbumin was common to other proteins. BMA was carbamylated as described above and 25 out of the 58 lysine residues were converted to homocitruilines [10]. The buoyant titration curves of the native and modified protein were measured and are given in fig. 17.

The high pH $\Delta\rho$ for the modified protein is seen to be only 0.034 g/ml in contrast to the increment of 0.058 g/ml observed for the native protein. A much higher residual density is noted for this protein than for ovalbumin. The contribution of the 25 modified lysines is seen to be (0.024 g/ml)/25 = 0.001 g/ml per residue modified in excellent agreement with the ovalbumin data. The contribution of the histidine residues was correctly predicted from poly(His) model compound data. Calculations similar to those made for ovalbumin indicate that the high pH $\Delta\rho$ observed for BMA is due to increased Cs^+ binding.

3.4.3. Carboxyl-modified bovine serum mercaptalbumin

The neutral glycineamide group was introduced into BMA by the addition of glycineamide and 1-ethyl-3-(3-dimethyl aminopropyl) carbodiimide hydrochloride [28]. Fifty-four out of the 100 carboxyl groups were thus neutralized.

The results of the buoyant titrations of the native and modified protein are shown in fig. 18. The ρ_0's of the modified protein are lower at all pH's than the native protein. After the titration of the carboxyl groups, this behavior is as expected because of decreased Cs^+ binding. The observed density increment of 0.011 g/ml for the modified protein between pH 2 and 6 is in good agreement with that predicted from the poly(Glu) data, 0.015 g/ml, on the basis of the 46 remaining titratable groups. Similarly, the observed $\Delta\rho$ for the native protein in this pH range, 0.031 g/ml, agrees nicely with the $\Delta\rho$ predicted from model compound data of 0.033 g/ml.

Two other approaches to this data were attempted to measure the contributions of the carboxyl groups in BMA to its buoyant density. In the mid-pH range of 6 to 9, the two curves differ by the roughly constant amount of 0.032 g/ml. If this difference is corrected for the 0.012 g/ml residual density difference caused by the introduction of 54 glycineamide groups, the resulting 0.020 g/ml density difference is in reasonable agreement with the predicted value of 0.015 g/ml

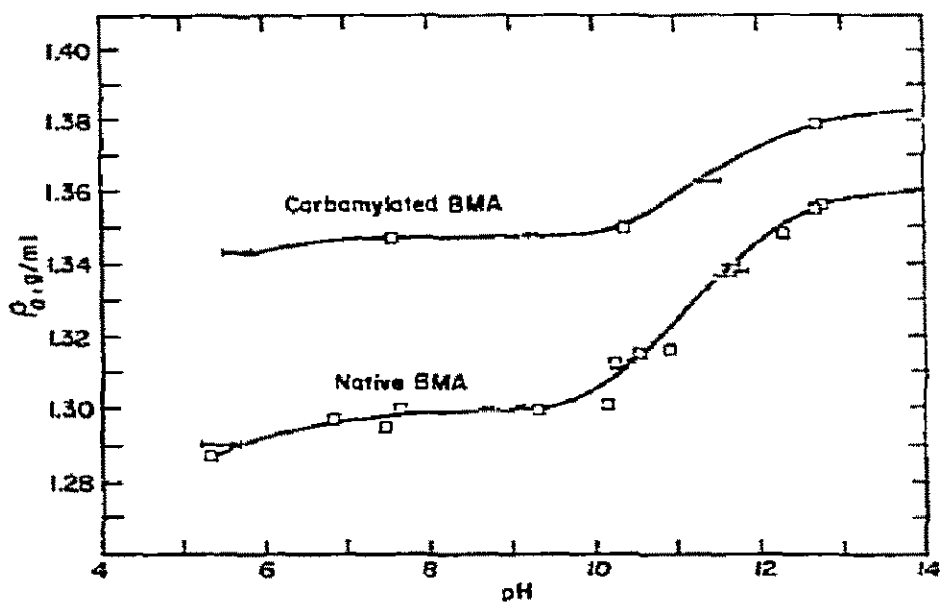

Fig. 17. Buoyant densities of native and carbamylated bovine serum mercaptalbumin as a function of pH; CsCl; 25°C. The arrows display the pH shifts with time, $pH_{initial} \rightarrow pH_{final}$. Runs involving no pH shifts are indicated by ▫ [10].

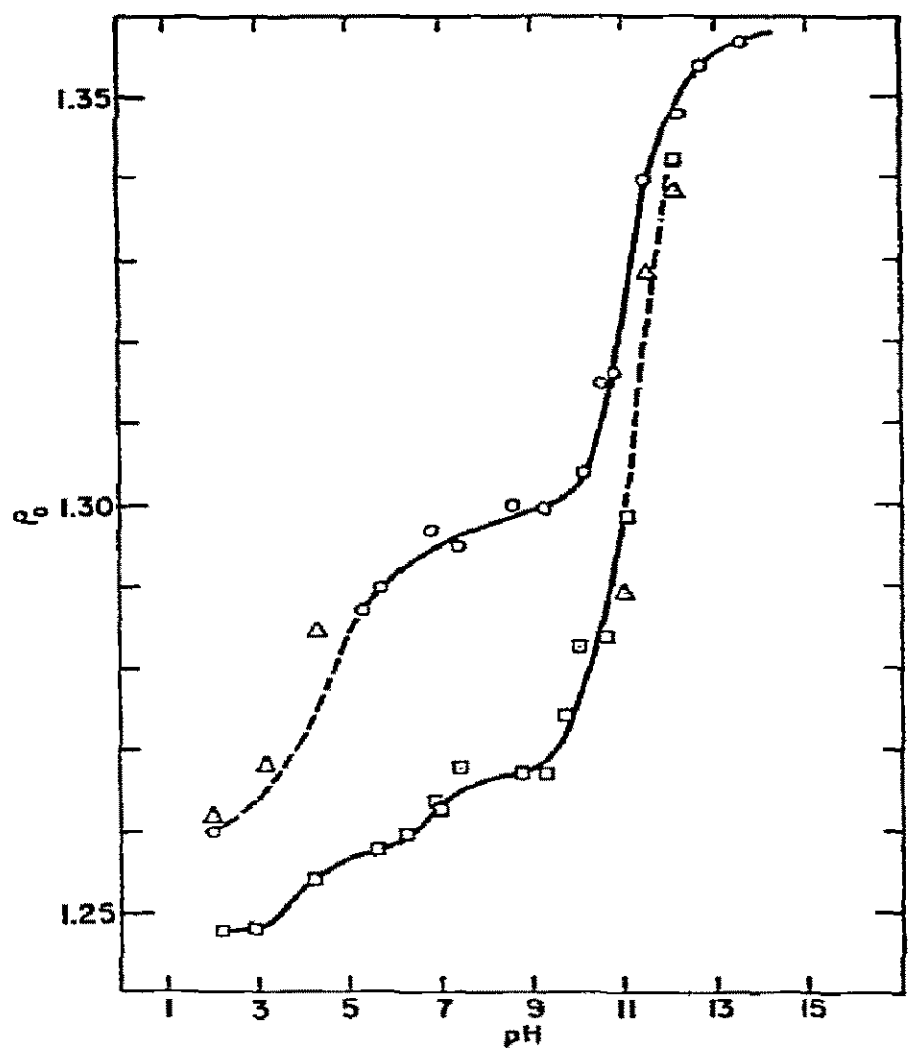

Fig. 18. Buoyant densities of native (○) and carboxyl-modified (▫) bovine serum mercaptalbumin as a function of pH; CsCl; 25°C [28]. Precipitates are indicated by (△).

obtained from model compound data. The other approach is to attribute the 0.032 g/ml density difference in the mid-pH range to the 54 neutral, modified carboxyl groups which are unable to ionize. This is equivalent to 0.0005_9 g/ml per carboxyl group titrated in good agreement with the value of 0.0006_3 g/ml per carboxyl obtained for ovalbumin [42].

It is apparent that a combination of studies of native and chemically modified proteins in density gradients in pH regions where the ionizable residues normally titrate and in the mid-pH range where no ionization occurs, will yield useful information as to the numbers of residues free to titrate, the pK's at which they titrate in concentrated salt solutions, and the contribution of each class of residues to the buoyant density of the native protein.

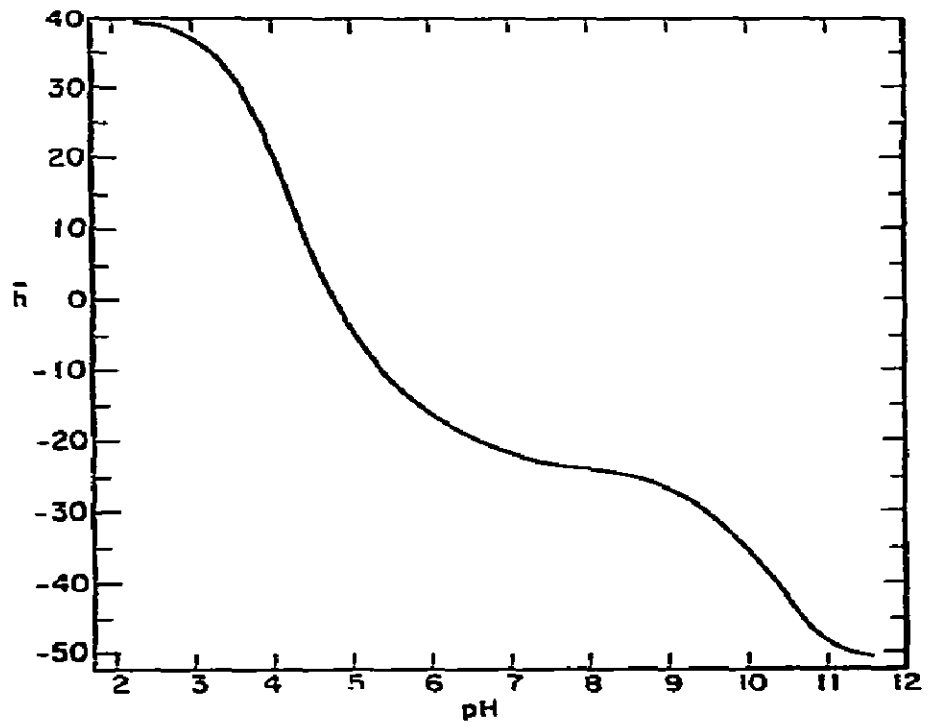

Fig. 19. The number of protons associated per molecule of isoelectric ovalbumin, $\bar{h}$, as a function of pH in 2.42 M CsCl at 25°C [41].

3.5. Correlative studies

It is apparent from the above discussion that the interpretation of buoyant densities and buoyant titrations of proteins is complicated by a variety of ion-binding, ionization and structural questions. In an effort to increase our understanding of the nature of the buoyant species, a number of ancillary investigations have been made. Potentiometric and spectropolarimetric investigations have yielded the most information to date.

3.5.1. Potentiometric titrations

The density increments occurring upon increases in pH are a reflection of ionization changes occurring in the molecule. In order to observe the primary effect, the actual deprotonation of the residues themselves, potentiometric titrations are necessary. We have found it necessary to conduct these studies ourselves because no potentiometric data are available for these polymers in concentrated CsCl solutions. Potentiometric titrations have been performed for two proteins, the six ionizable homopolypeptides and three of the five copolypeptides discussed earlier in this paper.

The potentiometric titration of ovalbumin in a buoyant CsCl solution was performed manually with a Radiometer pH meter [41]. The protein and blank solutions were titrated from the isoelectric pH with concentrated HCl and NaOH solutions in a micrometer syringe. The final protein concentrations were accurately determined by the Kjeldahl semimicro method of the Carlsberg Laboratory. From these data, the standard plot of $\bar{h}$, the number of protons dissociated per molecule of ovalbumin, as a function of pH was constructed. It is given in fig. 19. This curve is a fairly standard protein titration curve in that a large inflection occurs at pH 4.3 where the carboxyl groups ionize, the slope lessens noticeably in the mid-pH range where the small number (7) of histidines titrate and drops steeply again near pH 10 where the lysine and tyrosine residues titrate. The curve was analyzed in a standard way to reveal the inflection pH's which approximate the pK's and to yield the number of ionizable residues.

A sensitive test as to the relation between the potentiometric and buoyant data is to plot the degree of deprotonation, α, vs. buoyant density, ρ_0. This plot is possible because both variables are available as a function of pH. Fig. 20 displays this curve. The plot is linear from $\alpha = 0.05$ to $\alpha = 0.65$ which is the region in which the carboxyl groups titrate (pH 2.5 to pH 6.4). This indicates that a constant density increment occurs as each carboxyl group is deprotonated in turn affirming our assumption about the origin of the observed $\Delta\rho$ at low pH. The pronounced bump in the curve which begins at $\alpha = 0.65$ corresponds to the titration of the 7 histidine residues. This indicates that of the two proposals of Rasper and Kauzmann

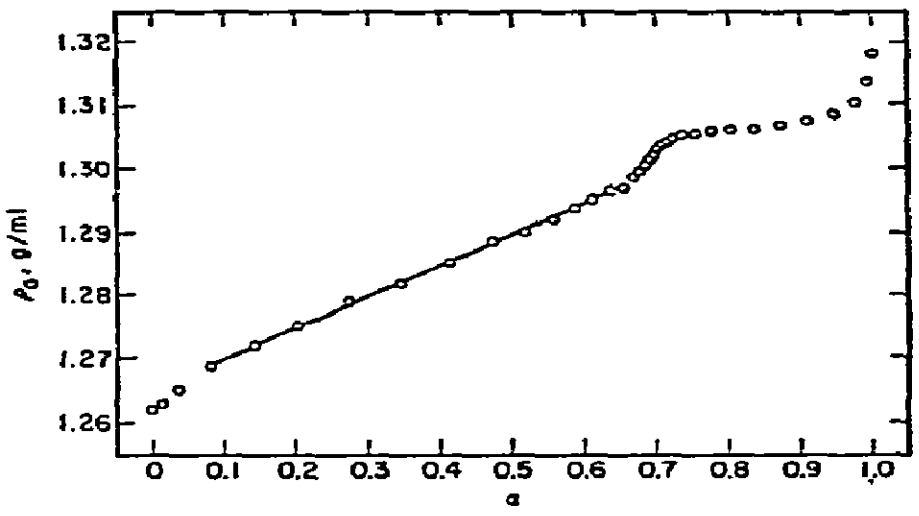

Fig. 20. The buoyant density, ρ_0, of ovalbumin as a function of the fraction of residues ionized, α, in CsCl solutions at 25°C [41].

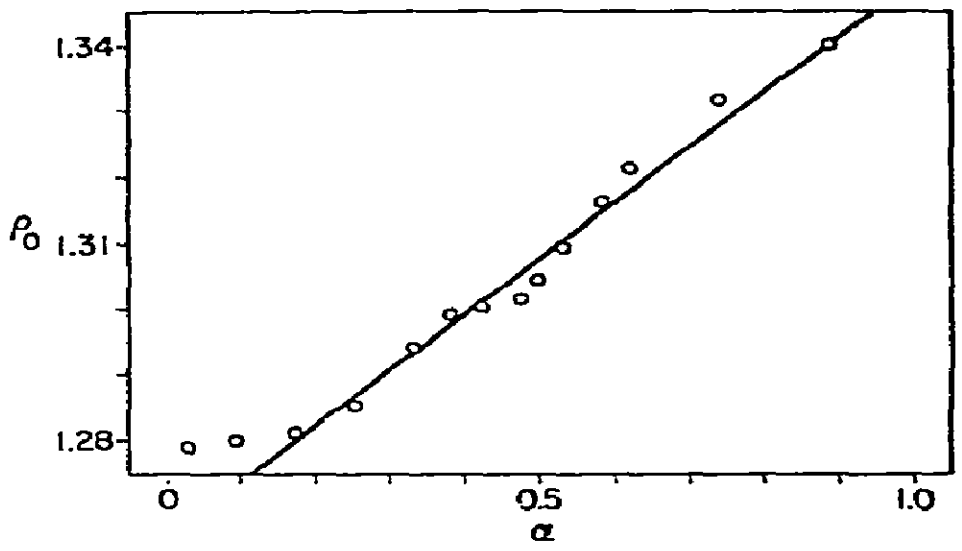

Fig. 21. The buoyant density, ρ_0, of human immuno-gamma globulin as a function of the fraction of residues ionized, α, in CsCl solutions at 25°C [29].

[42] to account for the abnormal volume changes in ovalbumin, the suggestion that the histidines titrate with an abnormally small volume change is correct.

Similar data were obtained for human IgG [29] to correlate with the buoyant density. Similar procedures were followed except that an automatic Radiometer Titrimeter system was employed to record the reference and protein curves in CsCl solutions. Concentrations were determined spectrophotometrically, α values computed as the fraction of groups deprotonated, and finally the α vs. ρ_0 plot shown in fig. 21 was obtained. This plot is substantially linear and has about the same slope as the ovalbumin plot.

Potentiometric titration curves in CsCl solutions were measured for the six ionizable homopolypeptides whose buoyant titration curves have been measured [35]. The results are given in fig. 22. These data confirm the buoyant titrations (fig. 12) as to the two classes of residues which titrate at about pH 5 and pH 10. The curves are not smooth and sigmoidal as would be expected for an ideal weak acid, primarily because of the phase transitions which all of these polymers experience as they are deprotonated in a concentrated CsCl solution. It is interesting to note that poly(Arg) titrates with a pK of 9.9 in CsCl as was found in the centrifuge studies.

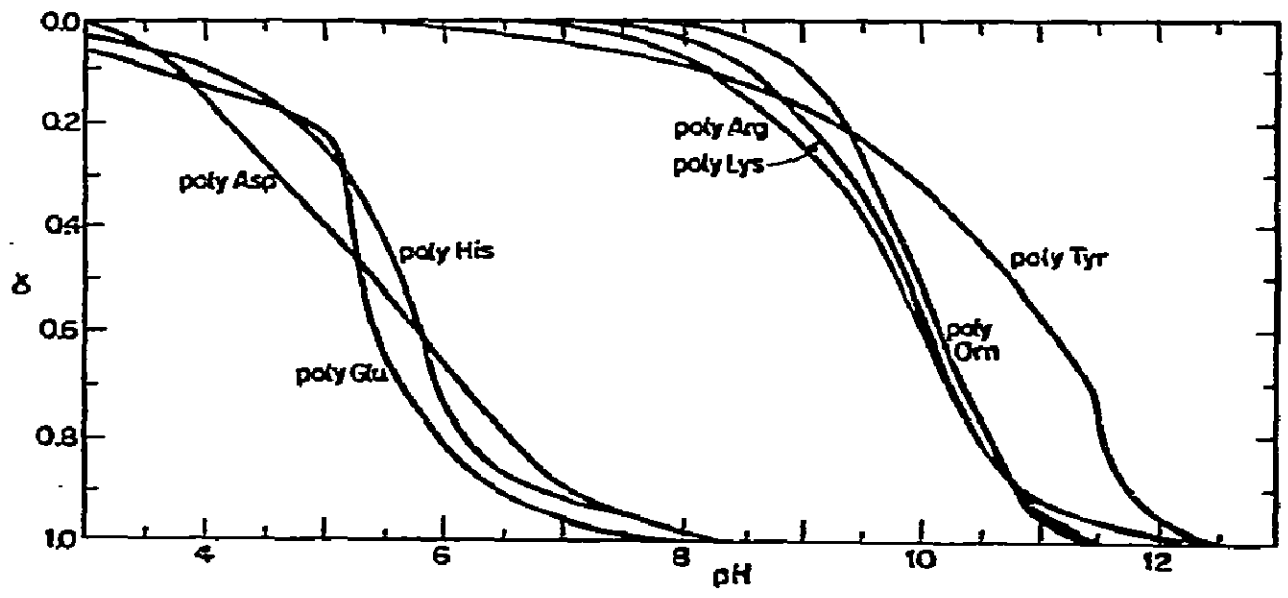

Fig. 22. The fraction of residues deprotonated, α, of seven homopolypeptides as a function of pH in CsCl solutions of buoyant composition at 25°C [35].

Table 7
pH at midpoint of transition

Homopolypeptide	Conc. CsCl [a]		Low Salt [b]
	Buoyant	Potentiometric	Potentiometric
poly(Glu)	4.5	5.3	4.5
poly(His)	5.6	6.0	6.1
poly(Arg)	10.0	9.9	13.0
poly(Orn)	9.3	10.0	–
poly(Lys)	9.5	10.0	10.4
poly(Tyr)	10.6	10.6	9.5, 11.5

[a] Ref. [35]. [b] Ref. [43].

Again the buoyant and potentiometric data were compared. A qualitative comparison is to simply compare the values of the two inflection pH's from the two titrations. Table 7 presents these data and indicates rather good agreement with the exception of poly(Glu). Again, the dichotomy for poly(Arg) is apparent from the value of pK_{int} reported by Fasman [43] for a low salt concentration.

ρ_0 vs. α plots were constructed for all homopolypeptides for which sufficient data were available from the buoyant titrations. Only the data in the region of the density transition is of any value in computing the ρ_0 vs. α plot. It is apparent from fig. 12 that the data for the modest inflections of the poly(Lys) and poly(Orn) ρ_0 plots are totally inadequate to generate a ρ_0 vs. α plot. The data for poly(His) are reasonably good and fig. 23 displays these ρ_0 vs. α values. It is obvious that the density change per unit ionization for the soluble, low pH form is markedly greater than that for the high pH, insoluble form. The same behavior was observed for poly(Glu).

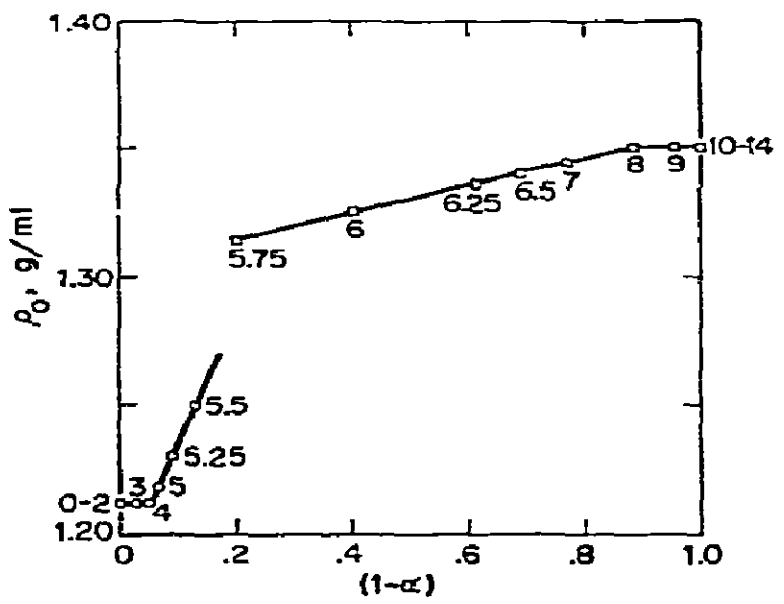

Fig. 23. The buoyant density of poly(His) as a function of the degree of deprotonation in CsCl at 25°C. (○) soluble; (□) precipitate. Numbers next to the data points represent the pH [35].

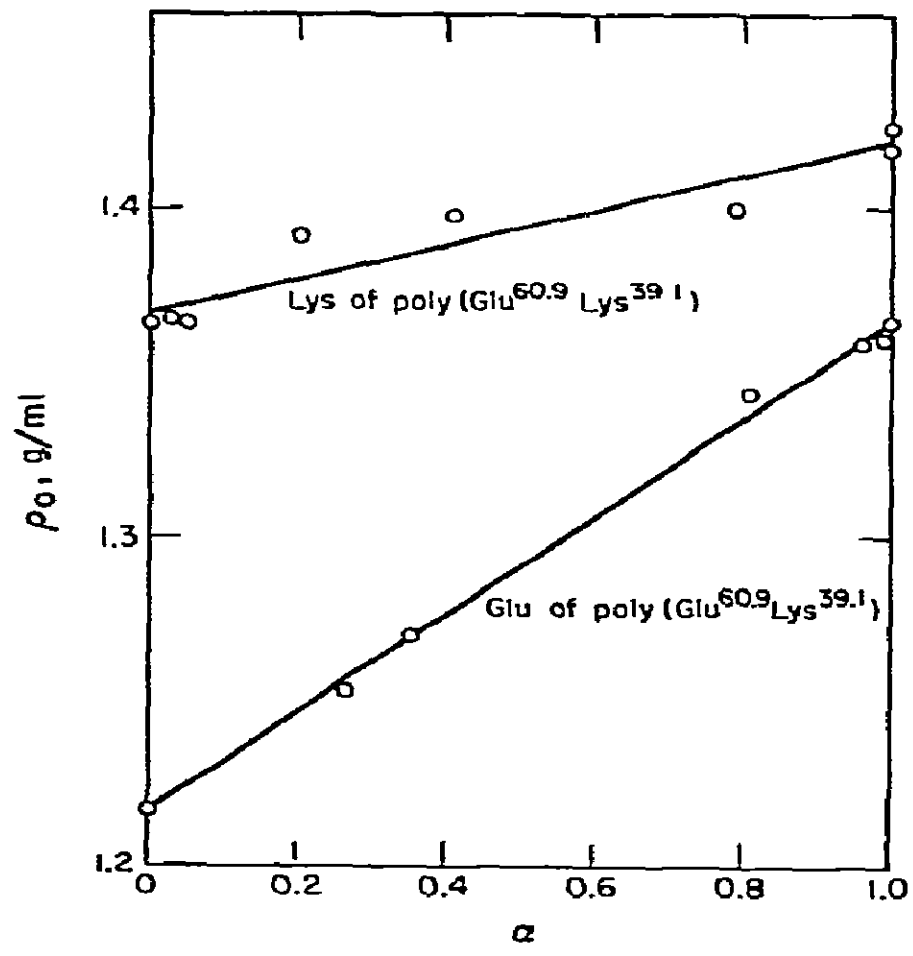

Fig. 24. The buoyant density of poly(Glu$^{60.9}$)(Lys$^{39.1}$) as a function of the degree of deprotonation of the glutamic acid and lysine residues computed separately in CsCl at 25°C [32].

Sharp et al. [32] measured the potentiometric titrations for several of the copolypeptides studied in density gradients. Fig. 24 shows that the α vs. ρ_0 plots for poly(Glu$^{60.9}$)(Lys$^{39.1}$), for each residue computed separately, are nearly linear. This linear dependence was also noted for the Glu residues of poly(Glu$^{54.5}$)(Tyr$^{45.5}$). These findings again substantiate that all buoyant density increments observed to date are the direct linear result of deprotonation of ionizable residues.

3.5.2. *Spectropolarimetry*

A serious concern about buoyant titrations and their interpretation is the structural integrity of the protein, especially at the extremes of the pH range. Again, we are faced with the problem of little or no data available on secondary and tertiary structural effects resulting from pH changes in buoyant salt solu-

tions. As in the case of the potentiometric data, we have had to generate this data in our laboratory.

The values of a_0 and b_0 for the Moffitt equation were measured from optical rotatory dispersion measurements for several proteins. The measurements were made with our newly-acquired Perkin–Elmer Model 241 spectropolarimeter which provides digital readout to 0.001° at 345 nm, 436 nm, 546 nm and 578 nm.

The rotation of BMA in buoyant CsCl solutions and in water was measured as a function of pH [44]. A value of $\lambda_0 = 218$ nm was used to compute the values of a_0 and b_0 given in table 8.

Although some conformational changes occur above pH 9, BMA is seen to retain most of its helical content up to the limits of the buoyant titration data, pH 12. Above pH 12, this protein appears to lose most of its helical structure. The data for the two solvents indicate that no major structural changes occur in going from H_2O to the buoyant CsCl solution.

The optical rotations at pH 7 of solutions of native and chemically modified (the glycineamide derivative) BMA were measured by Svendsen [28] in our laboratory as described above. The data were analyzed in terms of both the Drude and Moffitt equations. The results are given in table 9. The identical λ_c values for BMA in the four different states indicates that no major changes in the tertiary structure of BMA occur upon going from H_2O into CsCl or upon the formation of the glycineamide derivative. The b_0 values indicate some modest changes have occurred upon chemical modification. The $-[\alpha]_{578}$ data from the Drude equation and the a_0 values from the Moffitt relation indicate some moderate structural changes in changing solvents but no effects due to chemical modification.

Table 8
Moffitt parameters, a_0 and b_0, for native bovine serum mercaptalbumin in water and CsCl solutions as a function of pH at 25°C [a]

pH	In H_2O		In buoyant CsCl solutions	
	a_0	b_0	a_0	b_0
5.0	286	233	285	256
6.0	285	236	282	252
7.0	282	235	280	253
8.0	281	236	279	251
9.0	282	232	280	256
10.0	288	224	285	241
11.0	312	195	302	211
12.0	345	151	321	166

[a] Data are from ref. [44].

Table 9
ORD parameters for native bovine mercaptalbumin and mercaptalbumin modified at carboxyl groups [a]

	$-(\alpha)_{578}$	λ_c	$-a_0$	$-b_0$
Native BMA, literature	–	–	338	253
Native BMA, this study	65.4	265	328	248
Native BMA in CsCl	59.5	265	285	254
COOH-modified BMA	63	265	326	190
COOH-modified BMA in CsCl	56.4	265	270	200

[a] Data are from ref. [28].

These potentiometric and spectropolarimetric studies as well as the technique of high speed membrane osmometry continue to receive attention in our laboratory as we pursue our studies of proteins in density gradients at sedimentation equilibrium.

References

[1] M. Meselson, F.W. Stahl and J. Vinograd, Proc. Natl. Acad. Sci. U.S. 43 (1957) 581.
[2] M. Meselson and F.W. Stahl, Proc. Natl. Acad. Sci. U.S. 44 (1958) 671.
[3] N. Sueoka, J. Marmur and P. Doty, Nature (London) 183 (1959) 1429.
[4] C.W. Schmid and J.E. Hearst, Biopolymers 10 (1971) 1901.
[5] J.B. Ifft and J. Vinograd, J. Phys. Chem. 66 (1962) 1990.
[6] J.B. Ifft and J. Vinograd, J. Phys. Chem. 70 (1966) 2814.
[7] J.B. Ifft, in: A laboratory manual of analytical methods of protein chemistry, Vol. 5, eds. P. Alexander and H.P. Lundgren (Pergamon Press, New York, 1969) p. 151.
[8] J.B. Ifft, in: Methods in enzymology, XXVII, Part D, eds. C.H.W. Hirs and S.N. Timasheff (Academic Press, New York, 1973) p. 128.
[9] J.B. Ifft, in: Methods of protein separation: a modern survey, ed. N. Catsimpoolas (Plenum Publishing Corporation, New York, 1975) p. 193.
[10] D.A. Ellis, V. Coffman and J.B. Ifft, Biochemistry 14 (1975) 1205.
[11] J.B. Ifft, D.H. Voet and J. Vinograd, J. Phys. Chem. 65 (1961) 1138.

[12] J.B. Ifft, W.R. Martin III and K. Kinzie, Biopolymers 9 (1970) 597.
[13] C.L. Schildkraut, J. Marmur and P. Doty, J. Mol. Biol. 4 (1962) 430.
[14] J.E. Hearst and C.W. Schmid, in: Methods in enzymology, XXVII, Part D, eds. C.H.W. Hirs and S.N. Timasheff (Academic Press, New York, 1973) p. 111.
[15] R. Preston and J.B. Ifft, unpublished observations.
[16] K. Linderstrøm-Lang and H. Lanz, Jr., Compt. Rend. Trav. Lab. Carlsberg 21 (1938) No. 24.
[17] K. Linderstrøm-Lang, O. Jacobsen and G. Johansen, Compt. Rend. Trav. Lab. Carlsberg 23 (1938) No. 3.
[18] A. Hvidt, G. Johansen, K. Linderstrøm-Lang and F. Vaslow, Compt. Rend. Trav. Lab. Carlsberg 29 (1954) No. 9.
[19] J.E. Hearst, J.B. Ifft and J. Vinograd, Proc. Natl. Acad. Sci. U.S. 47 (1961) 1015.
[20] W. Bauer, F. Prindaville and J. Vinograd, Biopolymers 10 (1971) 2615.
[21] N. Fujita, K. Kinzie and J.B. Ifft, unpublished observations.
[22] J.B. Ifft, Compt. Rend. Trav. Lab. Carlsberg 38 (1971) 315.
[23] M. Mandel, in: Handbook of biochemistry, selected data for molecular biology, 2nd Ed., ed. H.A. Sober (The Chemical Rubber Co., Cleveland, 1972) H-9.
[24] D. Thorpe and J.B. Ifft, unpublished observations.
[25] J.W. Williams, K.E. Van Holde, R.L. Baldwin and H. Fujita, Chem. Revs. 58 (1958) 715.
[26] I.D. Kuntz, Jr., and W. Kauzmann, in: Advances in protein chemistry, Vol. 28, eds. C.B. Anfinsen, J.T. Edsall and F.M. Richards (Academic Press, New York, 1974) p. 239.
[27] A.E. Williams and J.B. Ifft, Biochim. Biophys. Acta 181 (1969) 311.
[28] I. Svendsen, in preparation.
[29] J.E. Ruark and J.B. Ifft, Biopolymers 14 (1975) 1161.
[30] J.S.V. Zil and J.B. Ifft, unpublished observations.
[31] G. Scatchard, J.S. Coleman and A.L. Shen, J. Amer. Chem. Soc. 79 (1957) 12.
[32] D.S. Sharp, R.J. Almassy, L.G. Lum, K. Kinzie, J.S.V. Zil and J.B. Ifft, Biopolymers, in press.
[33] R.V. Decker and J.F. Foster, J. Biol. Chem. 242 (1967) 1526.
[34] J.B. Ifft and A. Williams, Biochim. Biophys. Acta 136 (1967) 151.
[35] R. Almassy, J.S.V. Zil, L.G. Lum and J.B. Ifft, Biopolymers 12 (1973) 2713.
[36] E.J. Cohn and J.T. Edsall, Proteins, amino acids and peptides as ions and dipolar ions (Reinhold Publishing Corp., New York, 1943).
[37] N. Fujita, K. Kinzie and J.B. Ifft, unpublished observations.
[38] J. Vinograd and J.E. Hearst, in: Fortschritte der chemie organischer naturstoffe, XX, ed. L. Zechmeister (Springer-Verlag, Wien, 1962) p. 372.
[39] G.R. Stark and D.G. Smyth, J. Biol. Chem. 238 (1963) 214.
[40] I. Svendsen, Compt. Rend. Trav. Lab. Carlsberg 36 (1967) 235.
[41] J.B. Ifft and L.G. Lum, Compt. Rend. Trav. Lab. Carlsberg 38 (1971) 339.
[42] J. Rasper and W. Kauzmann, J. Amer. Chem. Soc. 84 (1962) 1771.
[43] G.D. Fasman, Poly-α-amino acids (Marcel Dekker, New York, 1967).
[44] J.A. Geleris and J.B. Ifft, in preparation.